Extending frequency and steering range of amplifier-antenna array via controlled mutual coupling

Jaanus Kalde

Aalto University

TARTU ÜLIKOOL · UNIVERSITY OF TARTU · 1632

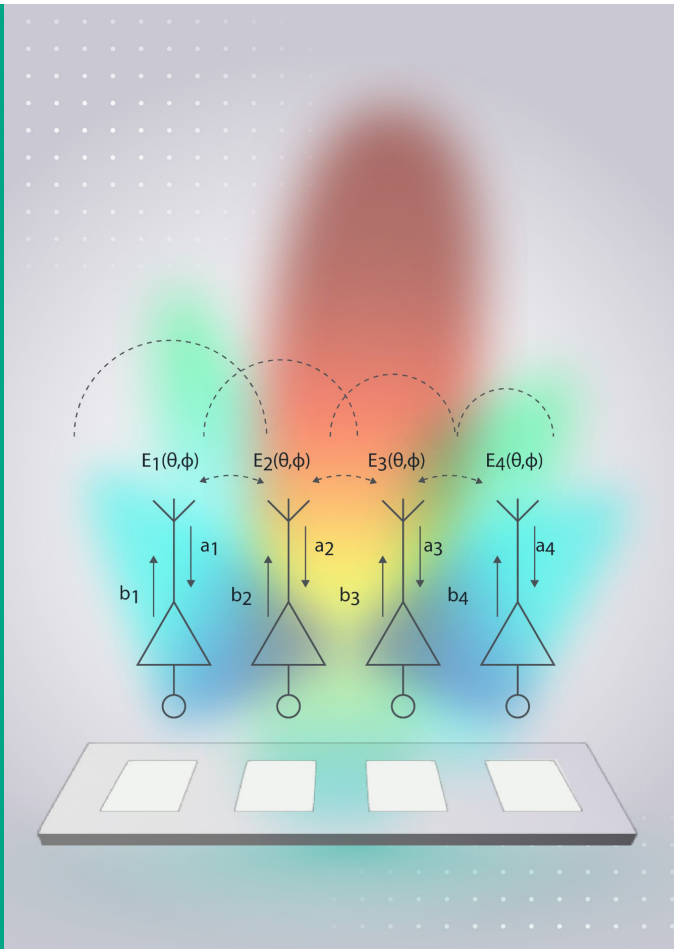

Aalto University publication series
Doctoral Theses 134/2025

Extending frequency and steering range of amplifier-antenna array via controlled mutual coupling

Jaanus Kalde

A doctoral thesis completed for the degree of Doctor of Science (Technology) to be defended, with the permission of the Aalto University School of Electrical Engineering and for the degree of Doctor of Philosophy (Physical Engineering), with the permission of the University of Tartu, Institute of Technology, at a public examination held at the lecture hall TU2 in Maarintie 8, Espoo on 22 August 2025 at 12.

Aalto University
School of Electrical Engineering
Department of Electronics and Nanoengineering

University of Tartu
Faculty of Science and Technology
Institute of Technology

Supervising professor
Prof. Ville Viikari, Aalto University, Finland
Prof. Alvo Aabloo, University of Tartu, Estonia

Thesis advisors
Dr. Anu Lehtovuori, Aalto University, Finland

Preliminary examiners
Prof. Joel Kuusk, University of Tartu, Estonia
Dr. Filipe Miguel Esturrenho Barradas, Instituto de Telecomunicações – Aveiro, Portugal

Opponent
Prof. Cyrille Menudier, University of Limoges, France

Aalto University publication series
Doctoral Theses 134/2025

Image on the cover: Kristjan Kalde

ISBN 978-952-64-2638-9 (paperback)
ISBN 978-952-64-2637-2 (pdf)
ISSN 1799-4934 (painettu / print)
ISSN 1799-4942 (pdf)

http://urn.fi/URN:978-952-64-2637-2

Unigrafia Oy
Helsinki 2025

Aalto University

ABSTRACT

Author Jaanus Kalde

Name of the doctoral thesis Extending frequency and steering range of amplifier-antenna array via controlled mutual coupling

Article-based

Number of pages 106

Keywords amplifier, antenna array, frequency bandwidth, mutual coupling, patch antennas, reconfigurable antenna

An increasingly connected world demands constant wireless communication and sensing innovation, particularly for next-generation technologies like 5G/6G and novel radars. Such systems require high-performance and reconfigurable radio frequency (RF) front-ends. This doctoral thesis develops a system-level design approach for antennas and amplifiers. The approach in this work is to utilise mutual coupling between antennas and amplifiers rather than trying to avoid and minimise it. Current research moves beyond a traditional component-centric view and adopts an integrated, co-design methodology.

The core of this thesis is a simulation framework that analyses coupled antenna arrays with their driving amplifiers, captures their interactions and includes the effects of feeding signals. A C-band pulsed power amplifier that uses GaN technology was developed [I]. The combinatorial feeding scheme [II] enables dynamic power combining and control directly in the air, eliminating the need for lossy power-combining circuits. This framework integrates antenna array modelling, nonlinear amplifier characterisation via load-pull, and a new iterative algorithm. This algorithm considers interelement coupling and nonlinearities and calculates each amplifier's active impedance. MATLAB's genetic algorithm was used to optimise signal phases fed to the amplifiers. A custom coupling circuit was used to control coupling levels between antenna elements to allow direct comparison. S-parameters, radiated power, and beam steering range were measured.

The system-level design approach demonstrated significant advantages. Studies confirmed frequency range broadening and improved beam-steering of an optimised system, especially at the steering range extremes [III]. To show its efficiency in combining power in the air, a combinatorial feeding scheme was validated [II]. A custom coupling circuit between the amplifiers and antennas resulted in a 92% increase in the operational frequency range in the broadside and a 36% increase in the frequency steer envelope [IV]. This thesis calls for a paradigm shift in RF system design. Substantial improvements in the frequency range, beam-steering, and power efficiency can be achieved if antenna arrays, amplifiers, and feeding signals are considered as an integrated whole. The framework is a powerful tool for designing future reconfigurable RF systems, implying that next-generation communication technologies and radars can be more adaptable, efficient, and compact.

Aalto-yliopisto

KOKKUVÕTE

Autor Jaanus Kalde

Doktoritöö nimi Võreantenni ja võimenditega süsteemi sagedusala ja kiire juhtimisala laiendamine vastastikuse sidestuse abil

Artiklipõhine töö

Lehekülgede arv 106

Märksõnad võimendi, võreantenn, sagedusala, vastastikune sidestus

Nõudlus tõhusate ja usaldusväärsete sidesüsteemide järele on tänapäeval üha suurem. Iga järgmine mobiilse side standardi põlvkond üritab teenindada rohkem kasutajaid kiiremini ja odavamalt ise sealjuures vähem energiat kulutades. Sarnast suundumust võib täheldada näiteks ka radartehnoloogia vallas, seda nii tsiviil- kui ka militaarrakendustes. Selliste süsteemide täpne analüüs ja optimeerimine nõuab aga terviklikku lähenemist, mis arvestab kõigi komponentide koosmõju. Käesoleva doktoritöö keskmes on terviklik meetod raadiosüsteemide analüüsiks. Erinevalt traditsioonilisest komponendikesksest lähenemisest keskenduti selles töös integreeritud süsteemidele. Lisaks seisneb käesoleva töö uudsus võreantenni elementide vastastikuse sidestuse vältimise asemel selle rakendamises, mille abil on võimalik jõudlust paremini optimeerida.

Töö keskmes on simulatsiooniraamistik, mis analüüsib suure sidestusega võreantenne ja juhtvõimendeid ning loob mudeli nende vastastik- ja sisendsignaalide mõjudest. Nimetatud raamistik ühendab järgmisi meetodeid: võreantenni modelleerimine, võimendite ebalineaarsuste iseloomustamine koormusmõõtmise abil ja võimendi näivtakistuse arvutamine algoritmi abil, mis võtab arvesse antenni elementide vahelist sidestust ja võimendite ebalineaarsusi. Välja töötatud raamistikku kasutati mitmete uurimuste läbiviimiseks, sealhulgas süsteemide analüüsiks, mis kasutavad kombinatoorset võimsuse liitmist. Tänu sellele lähenemisele, mis võimaldab dünaamilist raadiosignaalide kombineerimist õhus [II], on võimalik elimineerida kadudega võimsuse kombineerimise ahelad. Lisaks käsitleti töös ka GaN tehnoloogial põhineva uudse mikrolaine impulss võimsusvõimendi arendust [I].

Välja töötatud terviksüsteemi arvestav disain oli edukas. Mõõtmised kinnitasid optimeeritud süsteemis sagedusvahemiku laienemist, seda eriti just kiire juhtimisvahemiku äärtes [III]. See on oluline, kuna süsteemi jõudlus on tavapäraselt kõige piiratum just juhtimisvahemiku äärealadel. Kontrollitud sidestuse rakendamine andis tulemuseks 92% sagedusvahemike suurenemise otsesuunas ja 36% sageduse ja suuna vahemike kombineeritud ühistööala suurenemise [IV].

Käesolev doktoritöö tõestab, et suuremat sagedusvahemikku, kiire juhtimise ala ja energiatõhusust on võimalik saavutada, kui käsitleda antenne, võimendeid ja juhtsignaale ühtse vastastiku sidestust arvestava süsteemina. Doktoritöö käigus väljatöötatud uudne raamistik on hea tööriist kohandatavate raadiosüsteemide arendamiseks, tänu millele on järgmise põlvkonna side ja radarid tõhusamad.

Abstract

An increasingly connected world demands constant wireless communication and sensing innovation, particularly for next-generation technologies like 5G/6G and novel radars. Such systems require high-performance and reconfigurable radio frequency (RF) front-ends. This doctoral thesis develops a system-level design approach for antennas and amplifiers. The approach in this work is to utilise mutual coupling between antennas and amplifiers rather than trying to avoid and minimise it. Current research moves beyond a traditional component-centric view and adopts an integrated, co-design methodology.

The core of this thesis is a simulation framework that analyses coupled antenna arrays with their driving amplifiers, captures their interactions and includes the effects of feeding signals. A C-band pulsed power amplifier that uses GaN technology was developed [I]. The combinatorial feeding scheme [II] enables dynamic power combining and control directly in the air, eliminating the need for lossy power-combining circuits. This framework integrates antenna array modelling, nonlinear amplifier characterisation via load-pull, and a new iterative algorithm. This algorithm considers inter-element coupling and nonlinearities and calculates each amplifier's active impedance. MATLAB's genetic algorithm was used to optimise signal phases fed to the amplifiers. A custom coupling circuit was used to control coupling levels between antenna elements to allow direct comparison. S-parameters, radiated power, and beam steering range were measured.

The system-level design approach demonstrated significant advantages. Studies confirmed frequency range broadening and improved beam-steering of an optimised system, especially at the steering range extremes [III]. To show its efficiency in combining power in the air, a combinatorial feeding scheme was validated [II]. A custom coupling circuit between the amplifiers and antennas resulted in a 92% increase in the operational frequency range in the broadside and a 36% increase in the frequency steer envelope [IV].

This thesis calls for a paradigm shift in RF system design. Substantial improvements in the frequency range, beam-steering, and power efficiency can be achieved if antenna arrays, amplifiers, and feeding signals are considered as an integrated whole. The framework is a powerful tool for designing future reconfigurable RF systems, implying that next-generation communication technologies and radars can be more adaptable, efficient, and compact.

Kokkuvõte

Nõudlus tõhusate ja usaldusväärsete sidesüsteemide järele on tänapäeval üha suurem. Iga järgmine mobiilse side standardi põlvkond üritab teenindada rohkem kasutajaid kiiremini ja odavamalt ise sealjuures vähem energiat kulutades. Sarnast suundumust võib täheldada näiteks ka radartehnoloogia vallas, seda nii tsiviil- kui ka militaarrakendustes. Selliste süsteemide täpne analüüs ja optimeerimine nõuab aga terviklikku lähenemist, mis arvestab kõigi komponentide koosmõju. Käesoleva doktoritöö keskmes on terviklik meetod raadiosüsteemide analüüsiks. Erinevalt traditsioonilisest komponendikesksest lähenemisest keskenduti selles töös integreeritud süsteemidele. Lisaks seisneb käesoleva töö uudsus võreantenni elementide vastastikuse sidestuse vältimise asemel selle rakendamises, mille abil on võimalik jõudlust paremini optimeerida.

Töö keskmes on simulatsiooniraamistik, mis analüüsib suure sidestusega võreantenne ja juhtvõimendeid ning loob mudeli nende vastastik- ja sisendsignaalide mõjudest. Nimetatud raamistik ühendab järgmisi meetodeid: võreantenni modelleerimine, võimendite ebalineaarsuste iseloomustamine koormusmõõtmise abil ja võimendi näivtakistuse arvutamine algoritmi abil, mis võtab arvesse antenni elementide vahelist sidestust ja võimendite ebalineaarsusi. Välja töötatud raamistikku kasutati mitmete uurimuste läbiviimiseks, sealhulgas süsteemide analüüsiks, mis kasutavad kombinatoorset võimsuse liitmist. Tänu sellele lähenemisele, mis võimaldab dünaamilist raadiosignaalide kombineerimist õhus[II], on võimalik elimineerida kadudega võimsuse kombineerimise ahelad. Lisaks käsitleti töös ka GaN tehnoloogial põhineva uudse mikrolaine impulss võimsusvõimendi arendust [I].

Välja töötatud terviksüsteemi arvestav disain oli edukas. Mõõtmised kinnitasid optimeeritud süsteemis sagedusvahemiku laienemist, seda eriti just kiire juhtimisvahemiku äärtes [III]. See on oluline, kuna süsteemi jõudlus on tavapäraselt kõige piiratum just juhtimisvahemiku äärealadel. Kontrollitud sidestuse rakendamine andis tulemuseks 92% sagedusvahemike suurenemise otsesuunas ja 36% sageduse ja suuna vahemike kombineeritud ühistööala suurenemise [IV].

Käesolev doktoritöö tõestab, et suuremat sagedusvahemikku, kiire juhtimise ala ja energiatõhusust on võimalik saavutada, kui käsitleda antenne, võimendeid ja juhtsignaale ühtse vastastiku sidestust arvestava süsteemina. Doktoritöö käigus väljatöötatud uudne raamistik on hea tööriist kohandatavate raadiosüsteemide arendamiseks, tänu millele on järgmise põlvkonna side ja radarid tõhusamad.

Preface

The work in this doctoral thesis has been carried out in the Department of Electronics and Nanoengineering, Aalto University School of Electrical Engineering and Institute of Technology, Faculty of Science and Technology, University of Tartu in 2021 - 2025.

I would like to thank my supervisor, Prof. Ville Viikari, for giving me this research topic and guiding me with my research. I am grateful to my supervisor, Prof. Alvo Aabloo, for allowing me to study and research and helping me navigate academia. I would also like to thank my advisor, Dr. Anu Lehtovuori, for helping me focus my research and keeping me on track with writing. I thank co-authors Dr. Veli-Pekka Kutinlahti, Erik Amor, Kalle-Gustav Kruus, and Veiko Dieves for their collaborative efforts.

Finally, I extend heartfelt thanks to my family – wife Elo and children Helemeel, Kaljo, and Malev – for their enduring patience, encouragement, and unwavering love, which have been invaluable throughout this educational endeavour.

Tartu, June 12, 2025,

Jaanus Kalde

Contents

List of publications

This thesis consists of an overview and of the following publications which are referred to in the text by their Roman numerals.

I J. Kalde, V. Dieves, K. -G. Kruus, E. Amor and A. Aabloo. Small, Economical and Power dense C-Band 350 W Pulsed Power Amplifier. In 19th Biennial Baltic Electronics Conference (BEC), Tallinn, Estonia, 2024, pp. 1-4, October 2024.

II J. Kalde, V. -P. Kutinlahti, A. Aabloo, A. Lehtovuori and V. Viikari. Combinatorial feeding to controlling and combining power on a coupled antenna array. In 17th European Conference on Antennas and Propagation (EuCAP), Florence, Italy, 2023, pp. 1-5, March 2023.

III J. Kalde, V. -P. Kutinlahti, A. Lehtovuori, A. Aabloo and V. Viikari. Leveraging mutual coupling in antenna-amplifier systems for increased reconfigurability. IEEE Journal of Microwaves, vol. 5, no. 1, pp. 59-67, January 2024.

IV J. Kalde, A. Lehtovuori, A. Aabloo and V. Viikari. Widening frequency envelope of an antenna-amplifier system with coupling structure. IEEE Access, Vol. 13, pp. 656-663, December 2024.

Author's contribution

Publication I: "Small, Economical and Power dense C-Band 350 W Pulsed Power Amplifier"

The author is the main writer of the paper. The author and co-author K.-G. Kruus designed and manufactured the system. The author measured the system. This work was supervised by V.Dieves, E. Amor and Prof. Aabloo.

Publication II: "Combinatorial feeding to controlling and combining power on a coupled antenna array"

The author is the main writer of the paper and conducted the research himself. The work was based on research methods developed by V.-P. Kutinlahti. This work was instructed by Dr. Lehtovuori and supervised by Prof. Aabloo and Prof. Viikari.

Publication III: "Leveraging mutual coupling in antenna-amplifier systems for increased reconfigurability"

The author is the main writer of the paper and conducted the research himself. This work was instructed by Dr. Lehtovuori and supervised by Prof. Aabloo and Prof. Viikari.

Publication IV: "Widening frequency envelope of an antenna-amplifier system with coupling structure"

The author is the main writer of the paper and conducted the research himself. This work was instructed by Dr. Lehtovuori and supervised by Prof. Aabloo and Prof. Viikari.

List of figures

List of tables

Abbreviations

5G 5th Generation Mobile Communication Technology

BJT Bipolar Junction Transistor

DOA Direction-Of-Arrival

DUT Device Under Test

EBG Electromagnetic BandGap

EIRP Effective Isotropically Radiated Power

GA Genetic Algorithm

GaN Gallium Nitride

GNSS Global Navigation Satellite System

HPA High-Power Amplifier

MIMO Multiple-Input Multiple-Output

MMIC Monolithic Microwave Integrated Circuit

PA Power Amplifier

PCB Printed Circuit Board

PUMA Planar Ultrawideband Modular Antenna

RF Radio Frequency

S-parameters Scattering parameters

SDR Software Defined Radio

TWT Travelling-Wave Tubes

VNA Vector Network Analyser

VSWR Voltage standing wave ratio

Symbols

Γ reflection coefficient

Γ_{active} active reflection coefficient

ϵ convergence threshold for iterative algorithm

ϵ_r relative permittivity

η_m matching efficiency

θ elevation angle

λ wavelength

σ electrical conductivity

ϕ azimuthal angle

ϕ_i angle of the feed signal to ith amplifier

a_i power wave into port i of a network

$a_{2,i}$ power wave into the output port of the i-th amplifier

B set of amplifier model functions

b_i power wave from a port i of a network

$b_{2,i}$ power wave from the output port of the i-th amplifier

E_i electric far-field for antenna array element i

E_{tot} total electric far field

f frequency

N number of elements/amplifiers

P_{in} power into an amplifier

P_{loss} dissipative power loss

P_{out} power output of an amplifier

S scattering matrix

t iteration index

$\tan \delta$ dissipation factor

Z impedance

Z_0 characteristic impedance

Z_a antenna impedance

Z_{active} active impedance

Z_g internal impedance

Z_{real} real part of impedance

1. Introduction

This thesis explores active antenna arrays driven by power amplifiers, investigating how antenna coupling, traditionally viewed as a challenge, can be leveraged to improve array characteristics. This introductory chapter provides the necessary background context for this research and outlines the main scientific contributions.

1.1 Background

In today's rapidly advancing technological landscape, the demand for efficient and reliable communication systems is greater than ever [2]. As society becomes increasingly interconnected, the need for high-speed data transfer, seamless connectivity, and energy-efficient solutions drives innovation in mobile communication networks [3]. Each new generation of mobile communication standards aims to serve more users with faster data rates while consuming less energy and reducing costs [4]. This evolution is not limited to communication systems alone; similar trends are observed in radar technology, where advancements are driven by the need for enhanced detection, tracking, and situational awareness in both military and civilian applications [5, 6, 7, 8].

The evolution of mobile communication networks has been marked by significant advancements in radio hardware and spectrum allocations [9]. Traditional high-power sector antennas, which have been the mainstay of cellular networks, are gradually being replaced by more complex phased array systems [10, 11, 12]. These systems offer improved performance and flexibility, allowing for better coverage and capacity. However, the increased complexity of these antenna-amplifier systems requires a deeper understanding and methodology to optimise their performance. This thesis aims to provide insights into the intricacies of these systems, contributing to the development of more efficient and effective communication networks.

Similar to the evolution of communication systems, radar technology has undergone significant transformations [13]. Early radar systems relied on single vacuum tube transmitters and mechanically steerable antennas, which were bulky and limited in capability [14, 15]. Over time, these systems

have evolved to incorporate solid-state amplifiers and electronically steered arrays, offering enhanced performance and flexibility [16]. Modern radar systems employ active electronically scanned array technology, particularly those used in space- and power-constrained applications. This allows for simultaneous tracking of multiple targets and improved reliability.

Modern radio systems demand reconfigurable radio architectures. This reconfigurability encompasses key aspects such as beam steering, frequency agility and output power control, enabling adaptation to diverse operational scenarios. The increasing demand for efficient data transmission has heightened the importance of wideband operation as communication systems continue to expand their frequency ranges to enhance throughput and overall performance [17, 18]. Additionally, steerable antenna systems require broad beam steering capabilities to accommodate various applications, such as satellite communications, radar systems, and next-generation wireless networks.

However, achieving such adaptability presents significant design challenges. Amplifier feed signals directly affect the active impedance of antenna elements, which in turn influences amplifier performance and efficiency [19]. The interaction between antenna elements and power amplifiers must be carefully managed to maintain efficiency and stability. Techniques, including adaptive impedance matching and dynamic load modulation, are being explored to address these challenges and optimise overall system efficiency [20, 21, 22].

Transmit power control is often essential in wireless communication and sensing applications. Adjusting transmit power can serve multiple purposes, including reducing interference with other wireless systems, optimising the energy-per-bit ratio in wireless links, preventing saturation or distortion at the receiver, limiting electromagnetic exposure for safety considerations, and minimising the detectability of signals in sensitive environments [23, 24].

Integrating high-power amplifiers (HPAs) in active transmitting arrays is essential for delivering microwave power, but isolators used to mitigate load-pull effects are bulky and lossy. Recent research emphasises the importance of predicting load variations and accounting for distortion in nonlinear regimes [25, 26], necessitating simultaneous circuit and antenna analyses. Load-pull effects, which can significantly alter amplifier behaviour and potentially lead to device failure, have been traditionally addressed using isolators. However, the limitations of isolators have spurred interest in alternative methods. It has been shown that varying antenna loads induced by coupling effects can significantly impact the radiation characteristics of active array antennas, leading to significant discrepancies in predicting sidelobe levels if these effects are neglected [27]. Furthermore, reflection at the PA-antenna interface has been identified as a key parameter for unifying mismatch and mutual coupling issues, leading to the development

of reflection-aware modelling and linearisation methods that demonstrate robust performance under diverse conditions [28]. These studies underscore the necessity of considering both circuit and antenna characteristics in the design of active transmitting arrays.

In 5G transmitters, mutual coupling and mismatch degrade linearity and efficiency. Therefore, advanced modelling techniques are crucial for accurate prediction and optimisation. System-level frameworks now integrate circuit and antenna models for precise interaction analysis [29, 30, 31]. Dual-input PA models address bidirectional signal flow, moving past simple 50 Ω loads. Validation via simulations and measurements confirms that impedance variations diminish performance across beam steering. Digital pre-distortion is explored to mitigate coupling-induced nonlinearities and improve efficiency [32]. This shows the need for coupling and mismatch modelling.

Active calibration techniques help to mitigate antenna coupling and PA mismatch in digital MIMO transmitters. These methods characterise individual RF chains and dynamically correct them for system variations [33]. Calibration demonstrably reduces error, improving signal fidelity and channel reciprocity. It ensures impedance adjustments do not induce distortions or reduce efficiency, stabilising transmitter operation [34]. These calibration approaches highlight the practical challenges of coupling and mismatch in antenna arrays.

1.2 Main scientific merits

The main scientific merits of this thesis are as follows:

1. Demonstrating that antenna systems with stronger mutual coupling provide more potential to optimise system performance by altering the signals fed to the amplifiers [III][IV].

2. Show that considering amplifier load-pull effects makes it possible to increase the system frequency band and steer envelope in coupled systems by feeding the amplifiers with signals, whose phase is optimised for the steer angle and used frequency [III].

3. Show that the coupling problem can be partially separable, by introducing a coupling network to an existing, low-coupling antenna array, resulting in increased system performance [IV].

4. Introducing a concept for enhanced power combining efficiency during sparse operation (PA switching) in coupled antenna array systems by actively leveraging antenna coupling [II].

2. Amplifiers and antennas in transmitters

This chapter details the simulation methodology developed and employed to analyse the behaviour of the coupled amplifier-antenna system. It describes the iterative approach used for active impedance calculation and discusses key practical considerations, including algorithm convergence, system stability, and the handling of measurement data.

2.1 Antenna design and modelling

In radio transmitters, antennas and amplifiers work together to transmit radio waves efficiently. Impedance matching between these components is needed for optimal power transfer. Individual antennas are passive devices that convert electrical signals into radio waves and vice versa. Multiple antenna elements are combined into antenna arrays to achieve desired radiation characteristics like beam steering and high gain. Fig. 2.1 illustrates a simplified radio transmitter with amplifiers driving an antenna array, visualising the generation of radiated electric fields from the antenna array. The figure also conceptually represents the mutual coupling between antenna elements and the flow of power between amplifiers and antennas in systems similar to those investigated experimentally in [III] and [IV]. There is a visual representation of waves between amplifiers and antennas, radiated electric fields and mutual coupling between antenna elements within this system. Mutual coupling describes the electromagnetic interaction between antenna elements, where the signal applied to one element induces currents and radiation in neighbouring elements, impacting the overall array radiation pattern. Understanding and managing mutual coupling is essential for predicting and controlling the overall radiation pattern of the antenna array system.

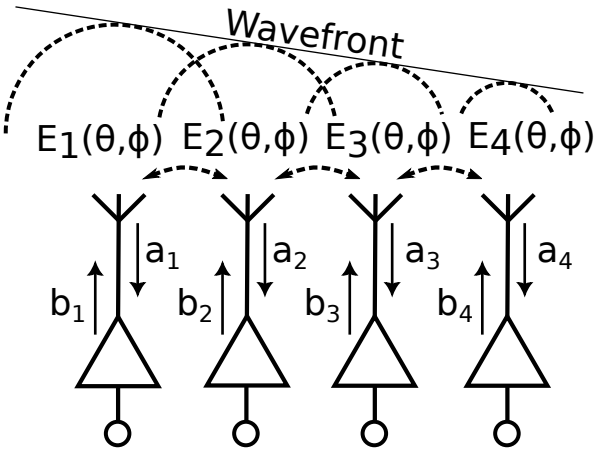

Figure 2.1. Simplified schematic of a radio transmitter with amplifiers connected to an antenna array.

2.1.1 Antenna impedance and coupling

The electrical impedance of the port and the interaction between ports can be described with a scattering parameter (S-parameter) matrix [35]. For example, the S-parameter matrix for two port antenna at a given frequency f would be:

$$S^f_{antenna} = \begin{bmatrix} S^f_{11} & S^f_{12} \\ S^f_{21} & S^f_{22} \end{bmatrix} \tag{2.1}$$

where S^f_{11} and S^f_{22} describe the impedance of ports one and two, respectively, and S^f_{12} and S^f_{21} the coupling between the ports. S-parameters of an antenna are frequency dependent, with each matrix corresponding to a point frequency. While coupling parameters could theoretically be zero, real antennas always exhibit some level of coupling between ports [19]. For example, the measured mutual coupling for the half-wavelength spacing patch antenna array used in the research [IV] is -22 dB, as illustrated in Fig. 2.2.

2.1.2 Antenna far-field radiation

Antennas transmit energy in the form of electromagnetic waves. These electromagnetic waves define the antenna's radiation characteristics. To understand the directional properties of an antenna, we consider its far-field radiation pattern. The far-field region is a distance sufficiently far from the antenna where the angular field distribution becomes essentially independent of the distance from the antenna. In this region, the radiation pattern describes how the magnitude of the electric field varies as a function of direction, represented by spherical coordinates (θ, ϕ).

For an antenna array, the total electric far field $E^f_{tot}(\theta, \phi)$ to a given direc-

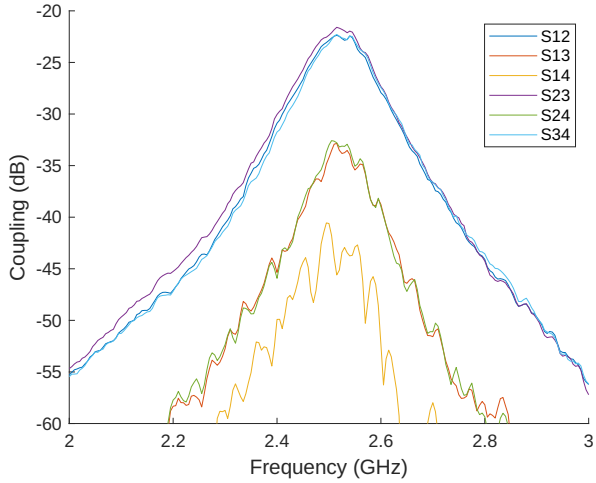

Figure 2.2. Mutual coupling of a four element half wavelength patch antenna array. [IV]

tion at a specific instantaneous point frequency f represents the overall radiation pattern [36]. This can be expressed as a sum of the individual element far-field patterns, $E_i^f(\theta, \phi)$, weighted by their respective excitation waves, $b_{2,i}^f$:

$$E_{tot}^f(\theta, \phi) = \sum_{i=1}^{N} E_i^f(\theta, \phi) b_{2,i}^f. \tag{2.2}$$

As depicted in Fig. 2.3, the total array pattern is formed by the combination of the individual element patterns. Since the element far-field patterns $E_i^f(\theta, \phi)$ are inherent to the antenna array design and can be considered fixed for a given array geometry and frequency, the primary way to control and shape the total far-field radiation $E_{tot}^f(\theta, \phi)$ is by adjusting the excitation waves $b_{2,i}^f$ applied to each element. By controlling the amplitude and phase of these excitation waves, we can steer the beam, focus energy, and achieve other desired radiation characteristics.

Mutual coupling between antenna elements in an array directly influences the array's overall radiation pattern. The currents induced in neighbouring elements due to mutual coupling modify the excitation waves and consequently alter the far-field radiation pattern compared to isolated elements. Therefore, understanding and controlling mutual coupling is critical for achieving the desired total far-field pattern and beam steering capabilities in antenna arrays.

2.2 Amplifier characterisation and active impedance

Amplifiers are essential components in radio systems, amplifying signals for radio transmission. Effective amplifier design and modelling are crucial for optimising system performance, particularly regarding efficiency and

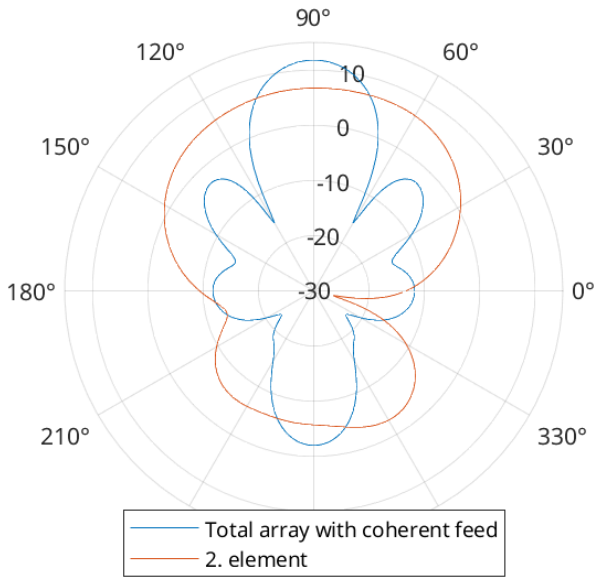

Figure 2.3. Simulated 2D polar plot of directivity patterns in dBi for the antenna array used in [IV]. The figure compares the pattern of a single representative element with the total array pattern achieved under coherent feeding.

stability. Furthermore, in antenna array systems, amplifiers are also vital for controlling radiation patterns and enabling beam steering. Therefore, careful amplifier design and accurate modelling are indispensable for high-performance radio transmitters.

2.2.1 Active impedance

Active impedance refers to the dynamic impedance experienced by an amplifier when connected to an antenna array, considering antenna mutual coupling, interactions within the system, and external influences. Unlike passive impedance, which remains constant, active impedance varies with feed signals, other amplifiers' state, or environmental conditions.

It is important to note that while "active impedance" is sometimes used in literature to specifically describe impedance conditions associated with $|\Gamma| > 1$, $\mathrm{Re}(Z) < 0$, or negative gain, its usage throughout this thesis refers specifically to the dynamic impedance at a port that varies depending on the operational state of the system, as defined above.

From an S-parameter and wave perspective, which aligns directly with measurement techniques, we can understand active impedance through wave quantities. For a multi-port antenna array connected to amplifiers, the relationship between amplifier incident waves a and reflected waves b is given by the S-parameter matrix [37]:

$$\mathbf{a}_2 = \mathbf{S}\mathbf{b}_2 \tag{2.3}$$

Specifically, for the i-th amplifier, the reflected wave $a_{2,i}$ is a combination

of contributions from the incident wave from all the amplifiers:

$$a_{2,i} = \sum_{j=1}^{N} S_{ij} b_{2,j} \tag{2.4}$$

The active impedance can then be calculated from these waves through the active reflection coefficient:

$$\Gamma_{active,i} = \frac{b_{2,i}}{a_{2,i}} \tag{2.5}$$

$$Z_{active,i} = Z_0 \frac{1 + \Gamma_{active,i}}{1 - \Gamma_{active,i}} \tag{2.6}$$

Understanding and managing active impedance is crucial for optimising amplifier performance in amplifier-antenna systems. It directly affects radiated power level, efficiency, stability, and overall system behaviour. Active impedance considerations are particularly important in systems with high mutual coupling between antenna elements, as these interactions can significantly alter the impedance seen by the amplifier.

In this work, as detailed in [III] and [II], active impedance and its effects on amplifiers are modelled by characterising the relationship between a and b waves using load-pull measurements and simulations and by developing models based on these wave quantities. The active impedance's dynamic nature, stemming from variations in operational conditions such as steering angle or feed configurations, captured by both theoretical formulations and experimental data, enables the development of more accurate models and optimises system performance under realistic operating conditions.

2.2.2 Concepts in amplifier modelling

Fig. 2.4 illustrates an amplifier model based on S-parameters, incident (a), and reflected (b) waves. A simplistic approach to modelling amplifiers involves using S-parameters and treating the loss between the amplifier's output reflection coefficient and the antenna's impedance as a mismatch loss. While this method is useful, it does not account for the amplifier's nonlinear properties or load variation, which can result in deviations from an impedance match. If mismatch loss alone were considered and plotted on a Smith chart against varying impedance, it would form a perfectly circular pattern centred around the matched impedance. However, when considering the amplifier's output power under load variation, the resulting pattern on a Smith chart is not always circular due to the amplifier's nonlinear behaviour and how load impedance affects its performance.

More advanced amplifier models, such as X-parameters, incorporate some nonlinearities and accurately represent amplifier behaviour [38]. However, a more detailed characterisation method is load-pull analysis. Load-pull characterisation is commonly used to determine how power-added efficiency,

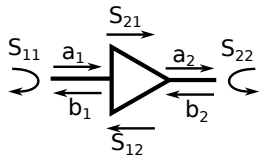

Figure 2.4. Amplifier model with S-parameters and waves.

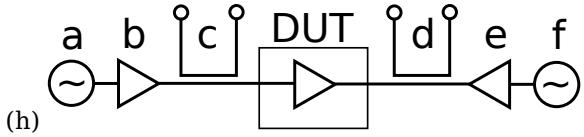

Figure 2.5. Block diagram of active load-pull measurement system. Signal generators (a,f) generate test signals for measurement amplifiers (b,e). Device under test (DUT) behaviour is measured with couplers (c,d).

gain, and maximum output power depend on impedance. This information helps in selecting the optimal operating impedance for impedance-matching networks.

2.2.3 Load-pull technique

Load-pull is a technique used to characterise and optimise the performance of amplifiers by measuring their behaviour under various load conditions. It involves systematically varying the impedance presented to the amplifier to identify the optimal load impedance for maximum power transfer, efficiency, gain or linearity [39, 40]. For characterisation with wideband signals, specialised techniques like two-tone or wideband load-pull are employed [41, 25, 26].

Load-pull measurements are conducted using specialised systems like the Maury Microwave MT2000 active load-pull system. The process involves connecting a measuring coupler and measurement amplifier to both the input and output of the amplifier under test, as shown in Fig. 2.5. Signals are generated and iteratively adjusted until the desired measurement impedance is achieved. This process is repeated for each desired input or output impedance point, allowing for a broad range of impedances to be measured.

Load-pull analysis provides insights into how output power, power-added efficiency, and gain depend on impedance. This information helps select the optimal impedance for impedance-matching networks, ensuring that amplifiers operate efficiently under real-world conditions. This information can help build models to predict amplifier behaviour when active impedance changes the amplifier load.

With an active load-pull measurement system, it is possible to measure load impedances inside and outside the Smith chart. The measurement capabilities are only limited by the maximum power of the measurement

amplifiers or the potential destruction of the amplifier under test [42].

2.2.4 Load-pull measurements and amplifier model

To apply the load-pull technique for characterising amplifier behaviour and developing an accurate model, this research employed both simulations [II] and experimental [III] load-pull measurements. The experimental setup involved a Maury Microwave MT2000 active load-pull system [43]. This system measured a broad range of impedances, covering most of the Smith chart with sufficient measurement points to construct a reliable amplifier model. The active load-pull measurement system operates by connecting a measuring coupler and measurement amplifier to both the input and output of the amplifier under test. Signals are generated and iteratively adjusted using measurement amplifiers until the desired output impedance is achieved. This process is repeated for each test frequency and impedance point combination.

The simulation or measurement process generates a dataset of points, each corresponding to a specific frequency and impedance combination. Complex values representing incident (a) and reflected (b) waves are recorded for each data point. These data define two measurement result planes on the Smith chart: one plane for the complex a waves and another for the complex b waves. The reflection coefficient, $\Gamma = \frac{b}{a}$, defines the relationship between these waves. The magnitude, shape, and orientation of these complex planes are determined by the amplifier's characteristics. Fig. 2.6 illustrates the measured complex planes obtained from data reported in [III].

Representing measurement data as complex wave planes offers a direct approach, mitigating potential issues of alternative representations. While conversion to magnitude and phase is possible, it introduces data conversion steps that risk errors. Furthermore, using magnitude and phase components directly presents challenges due to phase wrapping. This phenomenon, inherent to the cyclical nature of the phase, can complicate interpolation and optimisation algorithms, which may not inherently handle the discontinuity at the +/-180° (or 0°/360°) phase boundary. By maintaining the data in its native complex wave plane form, these conversion steps and phase-wrapping complexities are avoided. Interpolation and amplifier model development is based on these measured complex wave points and planes, ensuring data integrity and algorithmic robustness by working with the fundamental complex wave data.

Since the measurement points are discrete, while system simulations require continuous values for a_2, a two-dimensional interpolation is applied to the complex measurement results. A natural neighbour interpolation method is used to minimise discontinuities that could destabilise the simulation. For data points outside the measured region, a nearest-neighbour

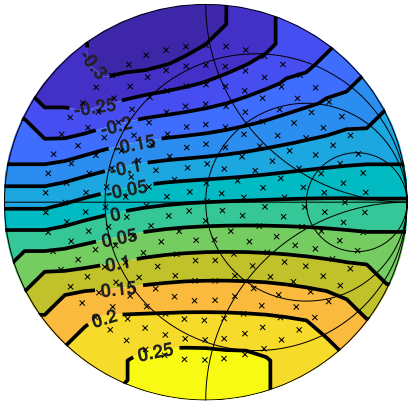

(a) Real part of incident wave (a) plane

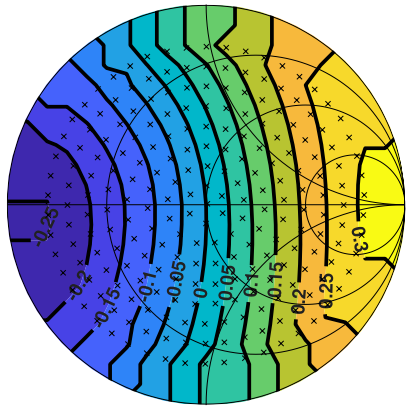

(b) Imaginary part of incident wave (a) plane

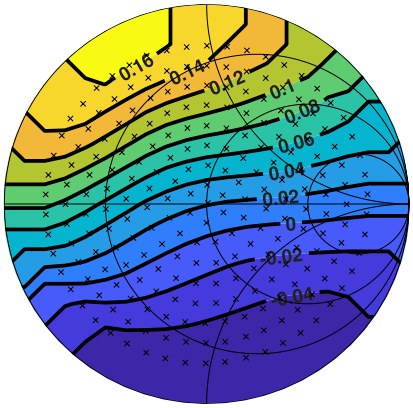

(c) Real part of reflected wave (b) plane

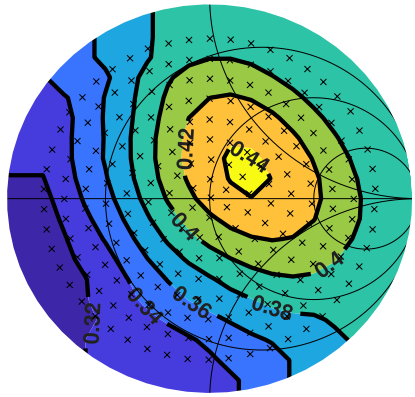

(d) Imaginary part of reflected wave (b) plane

Figure 2.6. Measured complex planes for incident (a) and reflected (b) power waves on the Smith chart. Measured points are marked with 'x', and the data are interpolated and extrapolated to create continuous planes.

extrapolation is performed. Additionally, a warning is displayed during system simulation if extrapolated data are used, as the amplifier's stability beyond the measured region is not guaranteed.

From these interpolated a_2 and b_2 planes, obtained at specific input wave levels (a_1) and frequencies, a continuous amplifier behavioural model is constructed. This model mathematically represents the relationship between the amplifier's input wave (a_1), the reflected load wave (a_2), the frequency (f), and the resulting output wave (b_2), and can be expressed as the mapping:

$$b_2^f = B(a_1^f, a_2^f, f) \tag{2.7}$$

While not a closed-form formula, the operation of this model is implemented via an algorithm. This algorithm works by de-embedding a_1 phases from a_2 input, using the frequency-selected set of a_2 and b_2 planes to find the b_2 value corresponding to a given a_2 value, and then re-embedding the phase of a_1 into b_2. Derived from the measured or simulated load-pull data, this model captures the amplifier's nonlinear response and is used later in system simulations to determine amplifier behaviour for any combination of input signal and active load impedance.

Stability is another critical aspect of amplifier performance [44]. Power amplifiers are stable within a specific operating load region. For instance, the power amplifier used in research [I] is rated for a maximum voltage standing wave ratio (VSWR Ψ) of 5:1 [45]. However, the amplifier characterised in [III] was load-pulled up to a VSWR of 10, beyond which measurement was avoided to prevent damage to the amplifier. Some amplifiers are designed to be unconditionally stable, meaning they remain stable regardless of the connected load impedance within the Smith chart.

In practical applications, particularly in active load-pull measurement systems or antenna arrays with significant mutual coupling, the system may encounter impedances beyond those typically represented within the Smith chart. The theoretical edge of the Smith chart corresponds to a reflection coefficient of 1, indicating total reflection. From a wave perspective, this condition occurs when $|a_2| = |b_2|$. However, an active load-pull measurement system generates a-waves externally, enabling measurements in regions where $|a_2| > |b_2|$, corresponding to reflection coefficients with magnitude greater than 1 ($|\Gamma| > 1$). This situation can arise in antenna systems with high coupling and impedance mismatch in real-world scenarios. Consequently, encountering conditions where $|a_2| > |b_2|$ due to coupling, which fall outside the scope of unconditional stability defined for passive loads, requires dedicated system-level stability analysis and poses significant design and integration challenges.

2.3 Antenna-amplifier system simulation

In previous approaches, amplifiers were matched to a reference impedance, with any mismatch between the amplifier and antenna treated as a simple mismatch loss. However, beam steering influences active impedance and amplifier performance. Load-pull data provides a more comprehensive analysis of their joint operation [46, 47, 48], aiding in array antenna steering [49]. Prior research [50] examined mutual coupling in nonlinear antenna arrays using the method of nonlinear currents, offering insights into coupling effects.

In our simulations ([III], [II]), the objective was to maximise the total electric far field $E^f_{tot}(\theta, \phi)$ to a given direction at a specific instantaneous point frequency f. As previously defined in Eq. 2.2, the total electric far field for an antenna array is formed by the sum of individual element far-field patterns, weighted by their respective excitation waves. For optimal radiation in a desired direction, the phase of b^f_2 should be aligned, and its magnitude should be maximised. The excitation waves b^f_2 are controlled by the incident waves a^f_1, but their relationship is governed by the amplifier model.

The dependence of the reflected waves a^f_2 on the excitation waves b^f_2 and the antenna's S-parameters can be formulated as:

$$\mathbf{a}^f_2 = \begin{bmatrix} a^f_{2,1} \\ a^f_{2,2} \\ a^f_{2,3} \\ a^f_{2,4} \end{bmatrix} = \begin{bmatrix} S^f_{11} & S^f_{12} & S^f_{13} & S^f_{14} \\ S^f_{21} & S^f_{22} & S^f_{23} & S^f_{24} \\ S^f_{31} & S^f_{32} & S^f_{33} & S^f_{34} \\ S^f_{41} & S^f_{42} & S^f_{43} & S^f_{44} \end{bmatrix} \begin{bmatrix} b^f_{2,1} \\ b^f_{2,2} \\ b^f_{2,3} \\ b^f_{2,4} \end{bmatrix} = \mathbf{S}^f \mathbf{b}^f_2. \tag{2.8}$$

However, the amplifier is nonlinear, meaning its output b^f_2 is influenced by both the incident wave a^f_1 and the reflected wave a^f_2. This relationship is described by the equation $b^f_2 = B(a^f_1, a^f_2, f)$ which is derived from load-pull simulations or measurements.

The antenna scattering, far-field parameters, and amplifier load-pull results are input into the active load calculation algorithm. This algorithm iteratively determines the self-consistent operating point of the coupled amplifier-antenna system under different feed configurations. The overall flow of this algorithm is depicted in Fig. 2.7. Following the convergence of the algorithm, the calculated far-field of the system is then used to optimise the feed angles of input signals, maximising radiated power at the desired direction and frequency. From this, the best feeds are used to calculate the system's steering and frequency envelopes.

The active impedance calculation algorithm operates iteratively for each frequency and set of feed coefficients to find a self-consistent solution for the interacting amplifier and antenna waves. For a given frequency f the input wave vector $\mathbf{a}^f_1$ for the array is constructed using feed phases for

each element. Although the input power P_{in} is not directly considered by the algorithm, it is selected during the amplifier characterisation process. The algorithm seeks to find the self-consistent output wave vector $\mathbf{b}_2^f$ and load wave vector $\mathbf{a}_2^f$ by simultaneously satisfying the amplifier behavioural model and the antenna's scattering characteristics. The iterative process is initiated with an estimate for the load wave vector, $\mathbf{a}_2^{(0)}$, and proceeds as follows for iteration $t \geq 0$:

1. Calculate Amplifier Output: Using the current estimate of the load wave vector $\mathbf{a}_2^{(t)}$ and the fixed input wave vector $\mathbf{a}_1^f$, calculate the amplifier output wave vector $\mathbf{b}_2^{(t+1)}$ for each element using the amplifier behavioural model B.

2. Calculate Antenna Reflection: Using the newly calculated amplifier output wave vector $\mathbf{b}_2^{(t+1)}$, determine the corresponding reflected load wave vector $\mathbf{a}_2^{(t+1)}$ generated by the antenna array using the antenna S-matrix $\mathbf{S}^f$.

3. Convergence Check: Check if the solution has converged by comparing the output wave vector from the current iteration $(t+1)$ to that from the previous iteration (t). If the maximum absolute difference between corresponding elements is below a defined tolerance ϵ, convergence is achieved.

4. Iteration Update: If convergence is not achieved, increment the iteration counter $(t \leftarrow t+1)$ and return to Step 1. If a maximum iteration limit is reached before convergence, the algorithm is terminated.

This process continues until convergence is achieved or the iteration limit is reached.

2.3.1 Optimisation method

To determine the optimal feed angles for maximising radiated power in a desired direction, a genetic algorithm (GA) implemented in MATLAB was employed in this work ([II], [III], [IV]). Genetic algorithms are a class of evolutionary algorithms particularly well-suited for optimisation problems with discontinuous or complex search spaces, where traditional gradient-based methods may struggle [51]. In this context, the phase control of the amplifier input signals (a_1) is quantised in discrete steps (5.6° resolution in our setup), creating a discontinuous optimisation landscape [52]. Beyond genetic algorithms, other robust optimisation algorithms are also being explored to optimise amplifier driving signals. For example, a dual-input power amplifier search algorithm operates in outphasing or Doherty modes

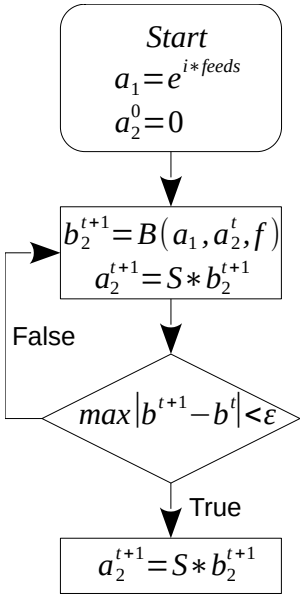

Figure 2.7. Flowchart of the active impedance calculation algorithm. [III]

to find optimal driving signals while maintaining high efficiency [53].

While GAs are powerful, they are known to potentially converge to local optima rather than the global optimum, especially in complex search spaces [54]. To mitigate this risk in our simulations, several strategies were adopted. Firstly, the search space was kept relatively small, and the search area was made sufficiently large to encompass a broad range of phase configurations. Secondly, the optimisation process was initialised with a progressive phase distribution, calculated based on ideal beam-steering principles. This provided a good starting point, guiding the GA towards promising regions of the search space and enhancing the likelihood of finding a near-optimal solution within a reasonable number of generations. The success of the GA in our research suggests that these measures were effective in finding suitable solutions for the phase optimisation problem within the defined constraints of our antenna-amplifier system.

2.3.2 Convergence and stability considerations

The active impedance calculation algorithm, depicted in Fig. 2.7, relies on an iterative process to achieve convergence between the interacting amplifier and antenna elements. In theory, iterative algorithms are not guaranteed to converge, and even if convergence occurs, it may not always be to a unique solution. These potential convergence issues were indeed encountered during the research detailed in [II] and [III].

To manage non-convergence, a failsafe mechanism was implemented in the simulation code. This mechanism monitors the number of iterations

and terminates the simulation with an error message if convergence is not achieved within a predefined iteration limit (set to 50 iterations in our case). In practice, simulations typically converged within 3-5 iterations under normal conditions. Non-convergence was observed in specific scenarios:

Firstly, the insufficient density of load-pull measurement points, combined with linear interpolation of the amplifier wave planes, leads to a highly non-smooth representation of amplifier behaviour. In such cases, the iterative algorithm could oscillate around a potential convergence point without ever reaching it, effectively circling the solution due to the irregularities in the interpolated amplifier model. Increasing the number of load-pull measurement points, as was done in [III] where 227 points were used, and employing natural neighbour interpolation helped to significantly mitigate this issue by creating smoother and more representative wave planes.

Secondly, convergence problems were also encountered when, due to high mutual coupling in certain antenna array configurations, the active impedance seen by some amplifiers ventured outside the boundaries of the Smith chart region covered by the load-pull measurement data. In these situations, the amplifier model relied on imprecise extrapolated data. This would sometimes lead to unstable iterations and non-convergence. To address this, an error was implemented to halt the simulation if the active impedance moved outside the measured Smith chart boundaries, ensuring the simulation operated within the validated amplifier model domain.

On a more fundamental level, the convergence of this iterative co-simulation algorithm is intrinsically linked to the inherent stability of the coupled amplifier-antenna system. Convergence essentially implies that the system reaches a stable equilibrium point in its operation.

While rigorous mathematical analysis of stability for such nonlinear iterative systems can be complex and delve into control theory beyond the scope of this work [55], a qualitative understanding of convergence speed and potential instability can be gained by considering the amplifier's large-signal output reflection characteristic. This characteristic, which relates the change in the reflected wave (b_2) to the change in the incident wave (a_2) in the large-signal operating regime (akin to a large-signal $\partial b_2/\partial a_2$), influences the damping of the iterative process. A smaller magnitude of this large-signal reflection characteristic contributes to faster convergence because the iterative updates are more strongly damped. This large-signal output reflection characteristic offers a valuable qualitative indicator for assessing potential convergence behaviour in these iterative co-simulations. The concept of unconditional stability, commonly defined for linear circuits connected to passive loads [56], does not directly apply to this large-signal iterative context.

3. Practical RF stability and coupling

This section explores two distinct areas: high-power amplifier stability and coupling effects within direction-finding systems. Understanding these effects is crucial for designing robust and reliable systems.

3.1 High-power amplifier stability

RF amplifier stability in high-power solid-state designs is crucial for performance and reliability. Achieving robust and predictable operation in practical scenarios involves mitigating factors that can lead to such instability or affect performance under varying conditions. Key challenges include instability caused by unwanted feedback paths. Unwanted feedback paths can arise from various sources and are commonly addressed using techniques such as isolation at the inputs and outputs of the amplifier, proper grounding, impedance matching, and the use of decoupling capacitors [57]. Additionally, more specialised methods like out-of-band feedback and control theory can be employed to further mitigate these issues [58, 59]. Furthermore, power reflection under load mismatch presents a risk to amplifier modules, affecting reliability and performance, particularly at high power levels. Optimised power combiners and isolators can help mitigate these issues [60]. Ensuring robust RF amplifier performance and stability requires integrating optimised design, feedback control techniques, and management of power reflection.

The practical significance of these stability considerations became evident during the development of a high-power C-band amplifier system [I]. While initial laboratory testing, performed under ideal conditions with resistive loads, successfully achieved the targeted 350 W output power, the transition to operational deployment revealed new challenges. Specifically, integrating a Vector Telecom VT58SGAH10NK antenna, characterised by a voltage standing wave ratio (VSWR) of up to 1.5 [61], introduced significant load variations. These variations, in turn, compromised the previously established system stability.

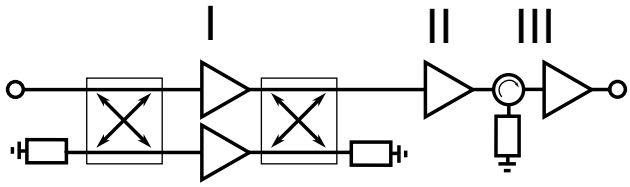

Figure 3.1. Block diagram of amplifier RF signal path, with stage numbers. [I]

Connecting isolators to the output of high-power amplifiers is a common practice to mitigate mismatch and coupling effects, ensuring stable and efficient operation. Isolators help protect amplifiers from reflected power due to load mismatches and improve overall system performance [62]. This was initially considered, and it was determined that this solution would reduce output power at the system output. Instead, an isolator (UIY UIYDI1220A5T6 [63]) was placed at an intermediate point, taking advantage of the available gain margin between the second and final amplification stages. This placement allowed system stability to be enhanced while maintaining output power levels. A gain budget analysis confirmed sufficient headroom, with power margins ranging from 2.6 to 3.4 dB across the amplification stages. The isolator's 0.5 dB insertion loss was accommodated without affecting the output power.

A primary scientific objective of this research [I], was the design and implementation of a high-power C-Band pulsed power amplifier capable of stable and efficient operation under varying load conditions. Achieving high efficiency was a key consideration, particularly in the context of pulsed operation and the significant quiescent power consumption of some amplifier modules. The design approach was validated through testing, and robust operation and stability were achieved across the 5.0 - 6.0 GHz frequency range. Output power measurements consistently exceeded the design target of 350 W, reaching at least 355 W (55.5 dBm) across all tested frequencies, as seen in Table 3.1. The gain at 350 W output shows some variation with frequency, notably requiring less input power at 5.2 GHz compared to other frequencies. This characteristic is observed in the measured data. This successful validation demonstrated that robust operation and stability were maintained with various antenna loads and during laboratory characterisation. Key factors contributing to this were the inclusion of the isolator and measures taken to minimise unwanted signal coupling between amplifier stages, specifically feedback of output power from one stage into an earlier stage through paths such as the amplifier circuits themselves, power supply circuits, or unintended electromagnetic coupling. These feedback paths were mitigated through careful layout, component selection, impedance matching, appropriate grounding, and decoupling techniques. These factors collectively contributed to a high-performing amplifier system.

Table 3.1. Measurement results. [I]

Frequency [GHz]	**5.0**	**5.2**	**5.5**	**5.9**	**6.0**
Small signal gain (P_{in} = -50 dBm) [dB]	56.6	57.4	59.6	56.3	54.9
Measured output power [dBm]	55.6	55.8	55.5	55.5	55.6
Input power (P_{out} = 350 W) [dBm]	2.8	-0.8	1.4	2	4.1
Large signal gain (P_{out} = 350 W) [dB]	52.8	56.6	54.1	53.5	51.5
Output power (P_{in} = 0 dBm) [dBm]	54.0	55.8	55.3	54.2	53.8

The primary scientific objective of this research was the design of an efficient solid-state high-power C-band pulsed power amplifier. The design approach was validated through testing, and stable operation was achieved across the 5.0 - 6.0 GHz frequency range. Output power measurements consistently exceeded the design target of 350 W, reaching at least 355 W (55.5 dBm) across all tested frequencies, as seen in Table 3.1. This successful validation demonstrated that stability was maintained with various antenna loads and during laboratory characterisation due to the inclusion of the isolator and careful attention to inter-stage coupling. These factors collectively contributed to a stable and high-performing amplifier system.

3.2 Coupling effects in direction-finding arrays

Beyond the realm of high-power amplifier stability, RF coupling manifests in diverse ways across different RF system architectures. Another critical area where RF coupling poses significant challenges is in direction-finding systems. In contrast to high-power amplifiers, where coupling primarily threatens stability, in direction-finding arrays, coupling between antenna elements directly impacts the accuracy of direction-of-arrival (DOA) estimation. This is particularly pronounced in cost-effective, affordable direction-finding systems where component tolerances and design constraints may exacerbate these effects. Therefore, understanding and mitigating inter-element coupling is crucial for achieving reliable and accurate DOA estimation. The following discussion shifts focus to explore these coupling effects within the context of direction-finding, drawing upon research conducted on affordable systems.

Earlier studies have highlighted comparable difficulties in calibrating antenna arrays and emphasise the need for accurate characterisation. They have proposed an innovative method for calibrating GNSS antenna arrays using live signals to address uncertainties and parameters that depend on the direction of arrival [64].

Furthermore, the design of antenna arrays itself presents opportunities for coupling mitigation. For example, employing dual-polarised antenna

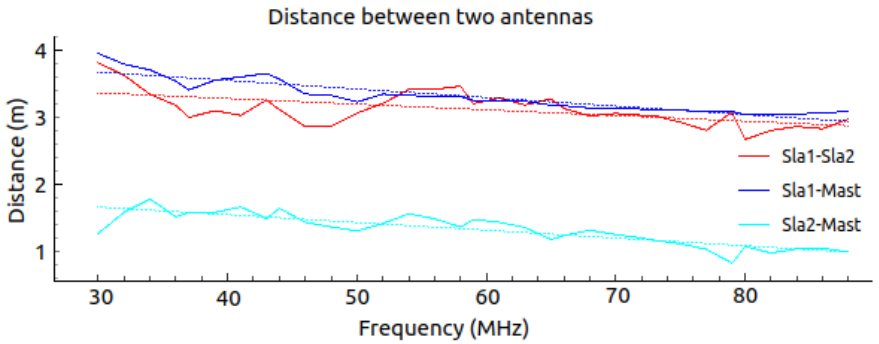

Figure 3.2. The calculated distances between the antennas that would give the smallest average error across all directions for different frequencies. (Reprinted with permission. [1])

arrays can reduce errors arising from polarisation mismatches [65]. This work highlights the importance of array geometry and element spacing in optimising direction-finding accuracy amidst mutual coupling.

Another manifestation of RF coupling challenges was encountered in research exploring affordable direction-finding systems [1]. In this specific investigation, conducted as part of a master's thesis project under the supervision of the author, focused on cost-effective solutions, a fixed antenna array comprising three closely spaced monopole antennas was examined. Due to the inherent characteristics of monopole antennas and their close proximity within the array, mutual coupling effects between antenna elements were observed. This coupling became a challenge, necessitating careful characterisation and compensation to achieve accurate direction-finding. Analysis revealed that despite the fixed physical spacing of 3.5 meters between antennas, the effective distance between these elements varied with frequency, exhibiting up to a 0.7 m variation over a 60 MHz frequency range. This frequency-dependent behaviour underscored the impact of mutual coupling in this antenna configuration.

This coupling effect was observed as a frequency-dependent virtual shrinking of the antenna array while its geometric proportions were maintained, as illustrated in Fig 3.2. Although the angular relationships between antennas remained relatively constant across the frequency range, the effective distances required frequency-dependent compensation. To address this challenge, specialised Python-based analysis tools were developed to process the complex phase relationships and unwrap the phase differences, enabling accurate characterisation of the system's behaviour under real-world conditions.

By analysing phase differences and determining best-fit parameters across various frequencies, a linear correction model for the antenna spacing was implemented. This compensation strategy was effective, and the direction-finding system, implemented using affordable software-defined radio (SDR)

hardware, demonstrated that even with significant coupling effects, proper characterisation and compensation could achieve reliable performance in real-world applications.

4. Coupled array power combining

There are several methods for controlling transmit power. One common approach is to adjust the input power to the power amplifier. However, this method often results in low efficiency when the amplifier operates in the back-off region, where the output power is significantly lower than the maximum capability [66]. To mitigate this issue, power can be combined from multiple parallel amplifiers, allowing each amplifier to operate at its optimal efficiency. This configuration involves switching amplifiers on and off to control the output power, but it requires additional power-combining circuitry that can introduce losses and occupy significant space on the chip or printed circuit board (PCB) [67].

The use of power-combining circuits presents several challenges. The active load impedance seen by the parallel amplifiers changes when amplifiers are switched on and off due to the coupling in the combining network. This variability in load impedance affects the efficiency and other properties of the amplifiers, making it difficult to maintain high efficiency across the entire output power range. To address these challenges, alternative methods have been explored, such as combining power directly on the antenna. An innovative example of this approach is the Doherty antenna, which combines the principles of the Doherty amplifier with antenna design, offering a relatively high linearity and efficiency suitable for signals with large amplitude variations [68, 69]. However, this approach may not be ideal for scenarios where multiple amplifiers are needed to generate adequate transmit power or where tunable output power is required. Prior research has explored the design and simulation of Doherty PAs within active antenna arrays, including investigations into the practical considerations and challenges of co-designing such integrated systems for efficient power-combining [69].

The antenna cluster concept uses multiple coupled radiators as a single antenna. By adjusting the phase and amplitude of the excitation signals, the active antenna impedance can be modified [70, 71]. This allows for additional impedance reconfigurability and power combining from multiple amplifiers without complex combining circuits. Furthermore, the array

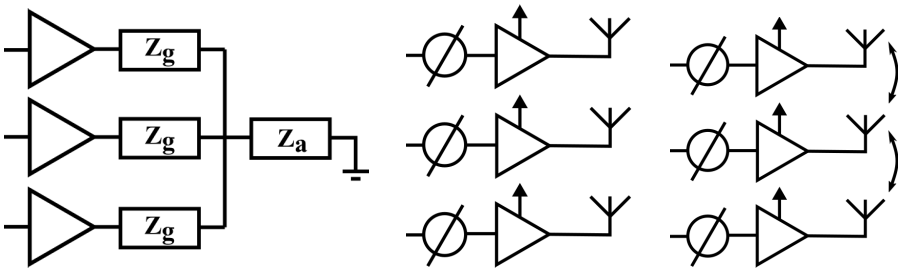

(a) Circuit-based combining **(b)** Uncoupled array **(c)** Coupled array system

Figure 4.1. a) Power combining schematic on circuit with amplifier impedance Z_g and load impedance of Z_a. b) Antenna amplifier system with uncoupled antenna. c) Antenna amplifier system schematic for coupled system with power supplies and phase shifters.

pattern of the cluster is less sensitive to the excitation signal weights compared to traditional antenna arrays. This makes it a promising candidate for output power control in coupled antenna elements [72]. Coupled antenna arrays offer advantages such as a wide operation band and a relatively large beam steering range. Examples of such arrays include the connected dipole array and the planar ultrawideband modular antenna (PUMA) [73, 74]. These arrays enhance performance and enable adaptive power combining from multiple amplifiers on the antenna, leading to more efficient and flexible wireless communication systems.

This chapter investigates power-combining techniques in coupled antenna arrays, employing active load impedance simulations to analyse the effects of mutual coupling and amplifier deactivation. The primary goal is to demonstrate a method for optimising power, combining efficiency and control in a multi-amplifier, coupled-antenna system, deviating from traditional approaches focusing on minimising coupling. This chapter presents the findings from [II], where a combinatorial feeding scheme for coupled antenna arrays was introduced. The system concepts discussed, including traditional circuit-based power combining and direct on-antenna combining in coupled arrays, are illustrated schematically in Fig. 4.1. It shows a schematic of circuit-based power combining (a), a simple amplifier connected to an uncoupled antenna (b) and the system configuration that is the focus of this chapter's investigation: multiple amplifiers feeding a coupled antenna array with controllable input signals and power supply (c).

Efficient power combining is crucial in many RF applications, from high-power transmitters to phased array systems. Traditional methods include circuit-based combiners (e.g., Wilkinson, Gysel) [35], which offer good isolation but can introduce losses and increase system complexity. Doherty amplifiers [75] provide high efficiency over a range of power levels but are typically designed for a specific power back-off point. Direct power combining on an antenna, as explored in one of the research papers in this

thesis, offers a potentially simpler and more compact solution, eliminating the need for dedicated combining circuitry. This approach aims to reduce system losses and size by integrating power combining directly into the antenna structure.

Antenna arrays are widely used for beamforming and spatial diversity. Conventional array design aims to minimise mutual coupling between elements to ensure predictable performance and independent control of each element [76]. Minimising mutual coupling simplifies array analysis and control but may limit performance in specific applications. However, recent research has explored the potential benefits of controlled mutual coupling. For example, tightly coupled arrays [77, 78] can achieve wider bandwidths by leveraging the interaction between elements; these designs often require more sophisticated analysis techniques to account for the complex impedance environment. Antenna clusters [79, 80] are another area of interest, offering frequency reconfigurability and beam steering flexibility through selective element activation and feeding strategies. In-antenna power combining methods are being explored for cluster-based approaches [79], while combinatory feeding methods have been demonstrated for reconfigurable antennas [80]. Building upon these concepts, the work presented here investigates how mutual coupling and active impedance considerations can enhance power combining efficiency and control. Furthermore, research has explored optimising EIRP by phase tuning in vector-modulator-driven arrays, highlighting the importance of impedance matching in array efficiency [81]. System-level analysis for efficient amplifier integration in arrays has also been emphasised in the design of compact GaN MMIC Doherty Power Amplifiers [82].

4.1 Active impedance simulation methodology

This section details the simulation methodology used to analyse the power-combining performance of a coupled antenna array with multiple amplifiers, some of which may be deactivated as used in [II]. The core concept is to accurately model the active load impedance seen by each amplifier, taking into account both the mutual coupling between antenna elements and the nonlinear behaviour of the amplifiers themselves. Accurately characterising the active load impedance is crucial for predicting the performance of power amplifiers in coupled array environments.

As discussed in Section 2.2.2 regarding amplifier modelling concepts, traditional S-parameter analysis is insufficient for modelling amplifiers operating in nonlinear regions or under varying load conditions, as is the case with power combining, where amplifiers may be switched on or off. S-parameters are linear, small-signal parameters that do not capture the large-signal, nonlinear behaviour of power amplifiers. Building upon this,

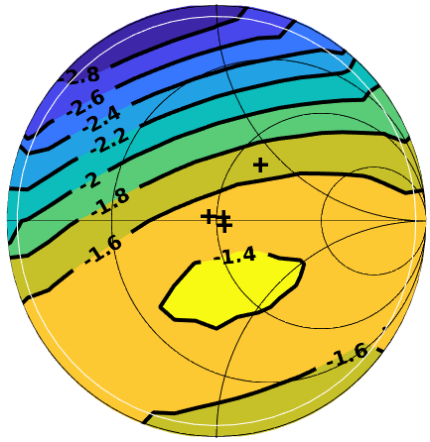

Figure 4.2. Simulated output wave (in dBm) of the amplifier over the load impedance at 2.5 GHz. The section outside of the white circle has been extrapolated. Antenna S-parameters are marked with + symbols. [II]

an improvement can be achieved by incorporating some nonlinear effects, such as X-parameters [83], which offer a more accurate representation of amplifier behaviour under varying drive levels. The importance of real-time impedance monitoring for adaptive amplifier control has also been demonstrated in power amplifier designs with integrated load impedance sensing [83]. Load-pull characterisation, on the other hand, is often employed to provide a more comprehensive understanding of amplifier behaviour across various loads, which can be used to inform such adaptive control strategies or simulations [84]. Load-pull measurements and simulations provide a detailed mapping of amplifier performance across a wide range of load impedances, capturing both linear and nonlinear effects.

A load-pull simulation of the amplifier output was performed, as in [II], to obtain a detailed behavioural model under a wide range of load impedances. Fig. 4.2 shows the measured load-pull data for the amplifier used in the simulations. The data encompasses the magnitude and phase of the output wave (b_2) for various load impedances presented to the amplifier, effectively mapping the amplifier's output power and efficiency as a function of load.

A crucial aspect of the combinatorial feeding scheme is the ability to deactivate amplifiers. A deactivated amplifier does not simply present an open circuit; it presents a complex impedance that depends on its internal structure and any residual biasing. A modified approach was used to model this, as detailed in [II]. The amplifier was turned off by disconnecting its bias voltage, but the amplifier circuit was still connected to the antenna. Instead of relying on a simple open-circuit model, a simulated signal was injected into the output of the deactivated amplifier. The reflected wave (both magnitude and phase) was then measured across a range of injected signal levels and phase angles. This process effectively characterises the input impedance by looking into the output port of the deactivated amplifier.

This data are then used to create a model of the deactivated amplifier that is comparable in format to the load-pull data of the active amplifiers. This detailed characterisation of deactivated amplifier impedance is essential for accurate simulation of power combining in arrays with amplifier switching.

An iterative algorithm implemented in MATLAB was employed to determine the operating point of each amplifier in the coupled array. This algorithm takes the antenna S-parameters, amplifier load-pull data, connection configuration, and input signal phase angles as input. The optimisation process had control over which amplifiers were turned on and off and the feed phase of each active amplifier. The iterative process accounts for the fact that the load impedance seen by each amplifier is affected not only by its own output but also by the signals from other amplifiers coupled through the antenna array.

4.2 Power combining performance results

The simulation framework described above was used to analyse the power-combining performance of the coupled antenna array under various feeding configurations. The key objective was to maximise the radiated power in the broadside direction while varying the number of active amplifiers.

Fig. 4.3 presents a comparison of three power-combining scenarios:

- **Theoretical Circuit Power Combining:** This represents the ideal power combining achievable with a lossless circuit-based combiner.

- **Simulated Radiated Power (Coupled Array):** This results from the active load impedance simulations using the iterative algorithm and the amplifier/antenna models described previously.

- **Theoretical Uncoupled Antenna Array:** This represents a hypothetical array where the elements are perfectly isolated, and the power combining efficiency is simply proportional to the number of active elements.

The results clearly demonstrate that the coupled antenna array, with optimised feeding, outperforms the uncoupled array in terms of power combining efficiency. This is because the mutual coupling, when properly managed, allows for a more favourable active load impedance to be presented to the amplifiers, even when some amplifiers are deactivated. The improvement is most significant when a small number of amplifiers are active. In the simulated case, the power combining efficiency is 44% higher than that of an uncoupled array when only one amplifier is active.

An alternative interpretation of these results is that a coupled array configuration yields a greater output power than a weakly coupled array,

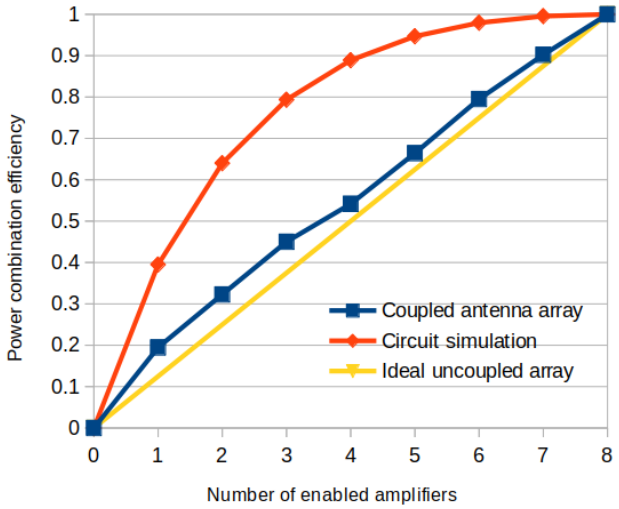

Figure 4.3. Theoretical circuit power combining, simulated radiated power density and theoretical antenna combining gain control against the number of enabled amplifiers. [II]

particularly when certain amplifiers are deactivated. This significant outcome demonstrates that even with amplifier deactivation, a coupled array can still attain superior power combining efficiency relative to an uncoupled array.

It is important to note that the specific shape of the power combining efficiency curve depends on the characteristics of the amplifiers and the antenna array (impedance, coupling levels, etc.). However, the general trend – that a coupled array can outperform an uncoupled array in terms of power combining efficiency – is a key finding of this research. The results also show that the optimal feeding configuration (which amplifiers are active and their relative phases) is not simply a uniform distribution. Instead, the genetic algorithm finds varied configurations that leverage the mutual coupling to achieve the best overall power combining. This non-intuitive feeding configuration highlights the complexity of optimising coupled array performance and the need for advanced optimisation algorithms.

A key scientific merit of this research, detailed in [II], is introducing a novel power control concept for coupled antenna array systems: dynamically switching the number of active amplifiers. This approach demonstrates the potential to enhance the performance of future antenna array systems by optimising power combining efficiency through active load impedance simulations. This method opens up new possibilities for designing efficient and flexible antenna arrays for various applications.

5. Coupling effects on frequency and steer envelope

This chapter examines the influence of mutual coupling levels on the performance of antenna-amplifier systems, specifically investigating its impact on the achievable frequency and beam-steering envelope. While traditional antenna array design prioritises minimising coupling for predictable element behaviour [85]. Common decoupling techniques to achieve element isolation include parasitic elements, electromagnetic bandgap (EBG) structures, and neutralisation lines [86, 87, 88, 89, 90], though these methods can introduce complexity and potentially limit bandwidth. Recent research highlights that controlled mutual coupling can offer performance advantages, such as enabling more efficient power distribution and improving radiation characteristics [91]. Examples like the connected dipole array [73] and planar ultrawideband modular antenna (PUMA) [74] demonstrate how utilising coupling effects can achieve wideband operation and enhance beam-steering performance.

Expanding the operational frequency range of antenna systems is often achieved through frequency reconfigurability. Traditionally, this involves using tunable circuits or elements to modify the antenna's frequency response [92, 93, 94]. These methods enable frequency switching via control signals but can introduce losses, distortions, and complexity due to the necessary biasing circuits and additional components [95].

An alternative approach to frequency reconfigurability leverages tightly coupled antenna arrays, intentionally utilising coupling effects to induce currents across multiple elements [96, 97]. This technique can enable ultrawideband operation, although it often presents a trade-off with the achievable beam-steering range. More recently, a method employing frequency-specific excitation of coupled antenna elements has emerged, allowing for dynamic frequency reconfiguration without physical switching [72, 98]. By applying tailored complex feed weights to each element, the system can dynamically adjust its operational frequency, offering broader bandwidth capabilities while maintaining reconfigurability.

Building upon these concepts, this chapter presents a combined simulation and experimental study, detailed in [III], to quantify the relationship

between coupling levels, frequency range, and steering capabilities. The research was conducted in two main parts: first, using a comprehensive simulation framework based on the active load impedance simulation method to predict system performance under varying coupling conditions; and second, experimental validation through constructing and measuring physical antenna arrays with different, well-defined coupling levels to confirm the simulation findings. The goal is to move beyond the conventional view of coupling as purely detrimental and explore its potential for enhancing system reconfigurability in terms of both frequency and beam steering.

This work builds upon these established concepts, ranging from traditional decoupling approaches to the exploitation of strong coupling in advanced array designs and reconfigurability through controlled excitation, by investigating the optimal coupling level for maximising the combined frequency and beam-steering range of a complete antenna-amplifier system, taking into account amplifier nonlinearities.

This work builds upon these established concepts, ranging from traditional decoupling approaches to the exploitation of strong coupling in advanced array designs and reconfigurability through controlled excitation, by investigating the optimal coupling level for maximising the combined frequency and beam-steering range of a complete antenna-amplifier system, taking into account amplifier nonlinearities.

5.1 Simulation and experimental methodology

Five distinct antenna array designs (labelled A-E) were created for the simulation study. All arrays consisted of four patch antenna elements in a linear configuration, designed for a centre frequency of 2.5 GHz, with a centre-to-centre element spacing of 40 mm (0.33λ). The arrays were designed on a 1.6 mm-thick FR-4 substrate, and the overall array dimensions were kept constant at 70 mm x 160 mm.

The primary design variable was the width of the patch elements, which directly controlled the mutual coupling between adjacent elements, as illustrated in Fig. 5.1. Narrower patches resulted in weaker coupling, while wider patches, with smaller edge-to-edge distance, increased the coupling. The lengths of the patches were slightly adjusted in each design to maintain an approximate resonance at 2.5 GHz. Table 5.1 summarises the key parameters of each array, including the coupling levels (S12) at the centre frequency, ranging from -18.5 dB (weak coupling) to -8.3 dB (strong coupling).

The amplifier used in the simulations was a custom-made design based on the BFP540 BJT transistor, matched to 2.5 GHz and operated in its nonlinear region (6 dBm input power, 3.3 V supply) to emulate realistic operating conditions. Its behaviour under varying load impedances was characterised

Table 5.1. Details of used antenna arrays [III]

Array label	A	B	C	D	E
Element spacing (mm)	14	4	1	0.5	0.1
Element width (mm)	26	36	39	39.5	39.9
Element length (mm)	27.7	27.5	27.5	27.5	28
Coupling (S_{12} (dB) @2.5 GHz)	-18.5	-12.7	-10.5	-10.1	-8.3
Coupling (S_{23} (dB) @2.5 GHz)	-16.9	-11.3	-9.5	-9.4	-8.8
Coupling (S_{13} (dB) @2.5 GHz)	-28.8	-21.8	-18.1	-15.5	-16.6

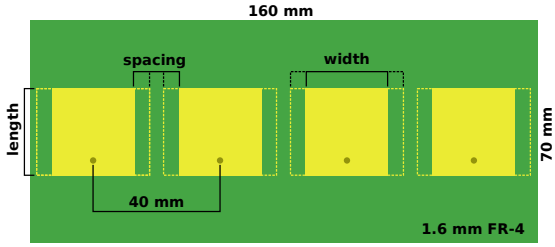

Figure 5.1. Illustration of antenna arrays. The width of the patches is modified to adjust mutual coupling. Array A (14 mm spacing) is displayed in filled colours, and array B (4 mm spacing) with dashed lines. [III]

using a Maury Microwave MT2000 active load-pull system, providing a comprehensive dataset of output waves as a function of load impedance.

The active impedance seen by each amplifier in the array was calculated using an iterative algorithm. This algorithm took into account both the antenna S-parameters (obtained from CST Studio Suite simulations) and the amplifier load-pull data. It iteratively calculated the output (b_2) and reflected (a_2) waves at each amplifier port, considering mutual coupling and nonlinear amplifier response, until convergence was achieved.

Finally, using MATLAB's genetic algorithm, system-level optimisation was performed for each antenna array design, frequency point, and steering angle. The optimisation goal was to maximise the radiated power in the desired direction by adjusting the feed signal phase angles to each active amplifier.

Two antenna arrays were selected and fabricated for experimental validation: Array A (weakly coupled, S_{12} = -18.5 dB) and Array D (strongly coupled, S_{12} = -10.1 dB). The measurement setup, shown in Fig. 5.2, included a RIGOL DSG3060 RF signal generator, a power splitter, three 6-bit phase shifters (5.6° resolution), and a Rohde & Schwarz FPH spectrum analyser. Measurements were performed in an anechoic chamber. A genetic optimisation algorithm, implemented in MATLAB, was used to maximise the radiated power in the desired direction by adjusting the phase shifters, mirroring the simulation procedure.

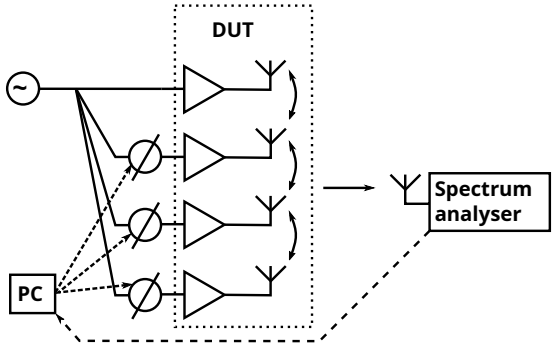

Figure 5.2. Setup used to measure system signal strength. [III]

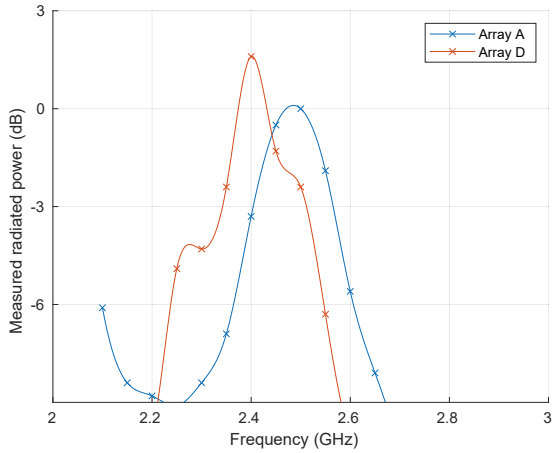

Figure 5.3. Measured radiated power in broadside direction over frequency. Measured points marked with x. Normalised to Array A maximum measured power level. [III]

5.2 Results and discussion

The simulation results revealed a consistent trend: increasing mutual coupling between antenna elements decreased the maximum radiated power at the centre frequency (2.5 GHz) but broadened the overall operational frequency range. The experimental measurements of Array A and Array D confirmed this trend. Fig. 5.3 shows the measured radiated power in the broadside direction over frequency. The coupled system (Array D) exhibited a 24% increase in the -6 dB frequency range compared to the weakly coupled system (Array A).

Furthermore, when beam steering was considered, the coupled system showed more than a 4 dB improvement in radiated power at certain frequency and steering angle combinations, particularly at the edges of the beam steering range ($> 55°$). The overall -3 dB frequency-steering envelope of the coupled system was found to be 41% larger than that of the weakly coupled system. These combined simulation and experimental

results demonstrate that minimising coupling is not always optimal, particularly when a large operating frequency and steering range are required. When combined with optimised feeding, the increased coupling enables the system to adapt its active impedance to maintain better performance across a wider range of frequencies and steering angles.

This work [III] provides compelling evidence for two key scientific merits. Firstly, it demonstrates the crucial role of amplifier load-pull effects in realising enhanced system frequency bandwidth and steering envelope in coupled antenna-amplifier systems. Secondly, and perhaps more significantly, the findings reveal that antenna systems with stronger, controlled mutual coupling offer greater potential for system performance optimisation when integrated with amplifier feeding. Combining active impedance simulations with realistic amplifier load-pull data and experimental validation provided strong evidence for this, demonstrating that controlled mutual coupling can be a valuable tool for enhancing system performance rather than being purely detrimental. These findings highlight the importance of a system-level design approach that considers the interplay between antenna coupling, amplifier characteristics, and optimised feeding signal phases, contributing to the development of more flexible and adaptable RF front-ends for next-generation communication and radar systems.

These results underscore that minimising coupling in antenna arrays may not always be the optimal strategy, especially when a wider operational frequency range and enhanced steering capabilities are the primary requirements. This highlights a key tradeoff between centre frequency performance and the achievable operational frequency/steering range that must be carefully considered based on specific system requirements.

6. Frequency and steering range with coupling circuit

This chapter investigates how mutual coupling affects amplifier-antenna systems' frequency range and beam-steering capabilities. Simulations and experiments quantify the relationship between coupling levels and these performance metrics [IV].

Previous research has explored methods to manage mutual coupling, including decoupling networks, metamaterials, and parasitic elements [86, 99]. The complex relationship between coupling and MIMO system performance has also been investigated, revealing that coupling can sometimes be beneficial [91]. Recent designs like small antennas and massive MIMO systems often exhibit inherent coupling [100, 101], leading to increased interest in understanding and potentially exploiting this phenomenon.

A controlled comparative methodology was employed to systematically investigate coupling effects in antenna arrays [IV]. A key challenge in previous studies was creating identical antenna arrays differing only in coupling characteristics, especially because active impedance varies with steering angle, making it difficult to isolate the effect of coupling alone. To address this, a novel coupling circuit was developed and implemented. Fig. 6.1 shows the reference system schematic, while Fig. 6.2 shows the system with the integrated coupling circuit.

6.1 Experimental setup

The experimental setup was designed to directly compare systems with and without the coupling circuit. Both used a four-element patch antenna array and custom amplifier, with the coupling circuit as the only difference.

6.1.1 System setup

The coupling circuit was designed to be inserted between amplifiers and the antenna array, allowing for controlled modification of the coupling level. It was fabricated on a custom PCB using commercially available directional

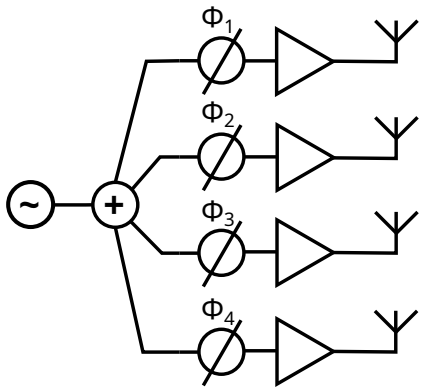

Figure 6.1. Schematic of the reference system. [IV]

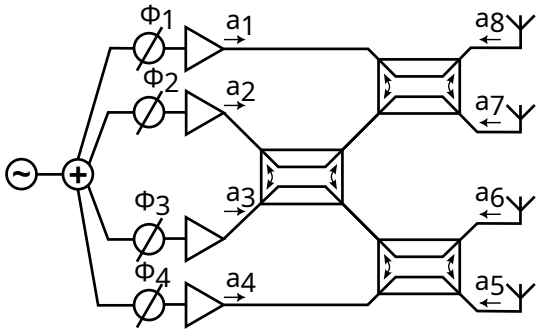

Figure 6.2. System with the coupler and the coupler schematic. [IV]

couplers (KYOCERA AVX CP0603A2442HNTR [102]). The PCB, measuring 187 mm x 20.6 mm, used a 1.5 mm FR-4 substrate and was designed to connect to the antenna array without cables. The schematic in Fig. 6.2 shows the configuration, where three directional couplers connect the four signal lines, replicating coupling between adjacent antenna elements and ensuring signal paths from amplifiers to antenna elements. The target was a -8.6 dB coupling level and up to 1 dB insertion loss, as per the directional coupler specifications [102].

Custom amplifiers, operating at 2.5 GHz and utilizing BFP540 BJT transistors, were used. The amplifier design was identical to previous work [III], operating in a non-linear region with 6 dBm input power and 3.3 V supply. A four-element linear patch antenna array, designed in CST Studio Suite for 2.5 GHz with half-wavelength element spacing and probe feeds, was used. The array was manufactured on a 1.5 mm FR-4 substrate. Element dimensions were 30 mm x 27.5 mm.

6.1.2 Measurement setup and system optimisation

The measurement system included a signal generator, power divider, four 6-bit phase shifters, custom amplifiers, and the four-port antenna array. The

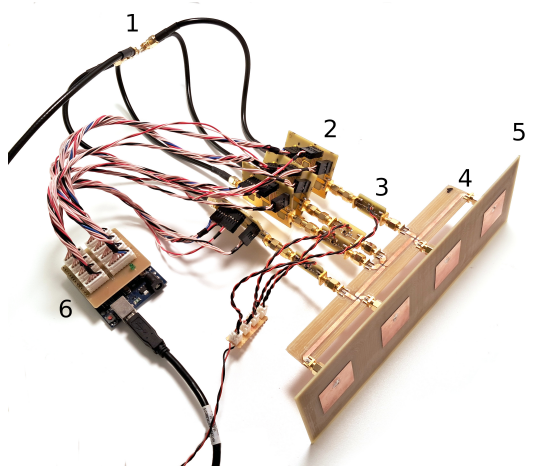

Figure 6.3. Photo of the device under test with power divider (1), phase shifters (2), amplifiers (3), coupler (4), antenna (5) and phase shifter controller (6). [IV]

main part of the measurement system and device-under test is illustrated in Fig. 6.3. Radiated power was measured using a separate antenna and a spectrum analyser. A MATLAB program with a genetic algorithm optimised the feed angles for each frequency and steering angle, maximizing radiated power. This optimisation was done for both the reference and coupled systems to ensure a direct comparison. Measurements were taken over the 2.3-2.6 GHz frequency range and for broadside, 15°, 30°, and 45° steering angles. Dissipation loss of the coupler was de-embedded from the measurements.

6.2 Experimental results

The experimental results in Fig. 6.4 demonstrate significant performance differences. The system with the integrated coupler exhibited a frequency range increase of at least 92% in the broadside direction. Additionally, a 36% increase in the overall -3 dB frequency range steering angle envelope was observed and is illustrated in Fig. 6.5. These findings indicate that controlled coupling can be strategically leveraged to enhance system performance rather than being universally detrimental.

Optimised feed angles (Figure 6.6) differed from progressive phase shifts. For the coupled system at broadside, central amplifiers had nearly opposite phase shifts to edge amplifiers (e.g., 0°, 112.5°, 112.5°, 22.5° at 2.5 GHz), suggesting a non-intuitive optimisation.

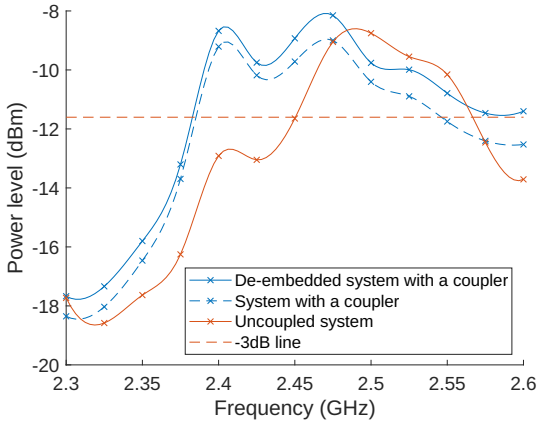

Figure 6.4. Measured and de-embedded radiated power levels at broadside for both the reference system and the system with the coupler. The measured points are marked with x's, and the connecting line is interpolated. [IV]

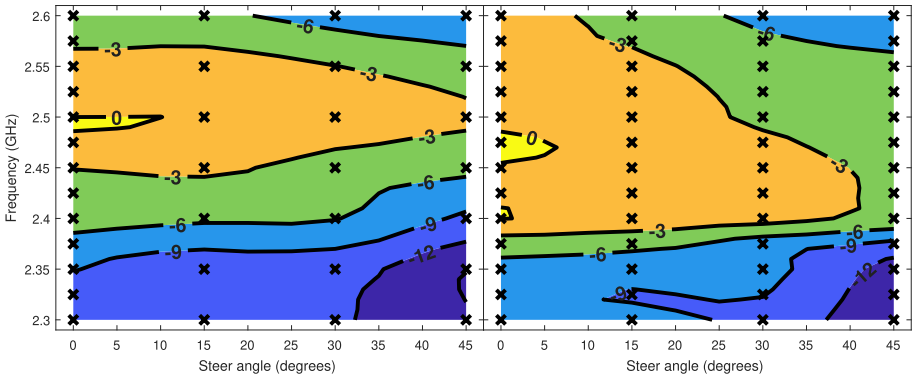

Figure 6.5. Comparison of measured radiated power over frequency and steer angle envelope for the reference antenna array (left) and the array with the coupler (right) in normalised dB. Measured points are marked with x, and the rest of the area is interpolated. [IV]

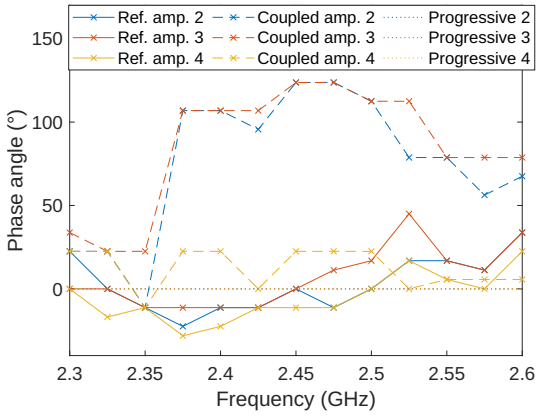

Figure 6.6. Progressive and optimised feed phase angles of reference and coupled systems over frequency range in broadside direction. [IV]

6.3 Discussion and conclusion

The primary scientific merit of this research lies in demonstrating that antenna systems with stronger, controlled mutual coupling offer significant potential for optimising system performance with amplifier feeding. This research provides a direct, controlled comparison of amplifier-antenna systems with and without enhanced coupling, using identical components except for the coupling circuit [IV]. The observed increases in frequency range and steering envelope demonstrate the potential of controlled coupling to improve performance. These findings challenge the traditional approach of minimising coupling, suggesting that, with careful design, it can be a valuable tool. Future work could investigate various coupling network topologies to further explore enhanced system performance.

7. Conclusion

The current doctoral thesis investigated the interaction between amplifiers and antennas in radio frequency systems, with a specific focus on antenna arrays that exhibit mutual coupling between elements. The research provided evidence that challenges the conventional design practice of minimising inter-element coupling. Through a combination of simulations and experimental measurements, the thesis demonstrated that strategically controlled mutual coupling paired with advanced amplifier modelling and optimised feeding signal phases could improve system performance.

The central contribution of this work was to develop and validate a system-level design approach. This approach went beyond the traditional component-focused perspective, where antennas and amplifiers are designed separately. The system-level design treated the antenna array, the driving amplifiers, and the signal feeding as integrated. A comprehensive simulation framework was created, which incorporated electromagnetic modelling of antenna arrays, non-linear characterisation of amplifiers through load-pull measurements, and an iterative algorithm to accurately calculate the active impedance presented to each amplifier. This algorithm was crucial: it accounted for both the mutual coupling between antenna elements and the nonlinear behaviour of the amplifiers under varying load conditions.

The thesis demonstrated the practical implications of this system-level approach through several key findings. Measurements using different antenna array configurations established that increased mutual coupling, combined with optimised feeding signal phases, can broaden the operational frequency range and enhance beam-steering capabilities, particularly at the extremes of the steering range. Knowing this, a custom-designed coupling circuit was implemented, allowing the control of coupling without modifying the radiating elements. Experiments with this circuit showed a substantial increase in the operational frequency range of the antenna-amplifier system: a 92% increase in the operational frequency range in the broadside and a 36% increase in the frequency-steer envelope. The concept of combinatorial feeding, where amplifiers were selectively activated and

their phases adjusted, was also validated, thus its potential for efficient power combining directly in the air and the mitigation of losses associated with traditional power-combining networks was demostrated. The design of a high-power pulsed amplifier showed the importance of considering amplifier behaviour under varying load conditions. This proved to be a key aspect of the overall system-level approach.

The results of this thesis suggest a reconsideration of established design principles in radio frequency systems. The work does not suggest that all mutual coupling is beneficial; it does, though, demonstrate that controlled coupling understood and managed on the system-level can significantly enhance performance. The developed simulation framework and experimental methodologies provide a pathway for designing future reconfigurable RF systems that are more adaptable, efficient and potentially more compact. The findings have relevance for the development of next-generation communication and advanced radar technologies to meet the continuously increasing demands for bandwidth, flexibility, and efficiency. The findings have relevance for the development of next-generation communication and advanced radar technologies to meet the continuously increasing demands for bandwidth, flexibility, and efficiency. This work thus lays a strong foundation for further exploration in active antenna system design.

Building upon the foundational system-level design approach established in this thesis, several promising avenues for future research emerge. A key direction lies in further exploring the relationship between antenna mutual coupling and amplifier performance to identify guidelines for optimal coupling levels. While this work demonstrated the benefits of controlled coupling, future studies could delve deeper into developing methodologies to predict or determine the ideal coupling characteristics for specific system requirements and amplifier types. This could involve correlating antenna S-parameters with amplifier load-pull data to provide practical insights for both antenna and amplifier designers, enabling them to co-design components for enhanced system performance rather than relying on separate, potentially conflicting, optimisation goals. For instance, future research could investigate how to interpret antenna impedance variations (derived from S-parameters, including the effects of mutual coupling) to inform desirable amplifier output impedance characteristics (derived from load-pull measurements) for optimal power transfer and efficiency across the operational bandwidth and scan range.

References

[1] E. Amor, “Design, testing and analysis of an affordable direction of arrival system using off-the-shelf SDR hardware and software,” Master’s thesis, Tartu Ülikool, Tartu, Estonia, 2022, supervisor: MSc Jaanus Kalde. [Online]. Available: http://hdl.handle.net/10062/83021

[2] W. Jiang, B. Han, M. A. Habibi, and H. D. Schotten, “The road towards 6G: a comprehensive survey,” IEEE Open Journal of the Communications Society, vol. 2, pp. 334–366, 2021.

[3] P. Yang, Y. Xiao, M. Xiao, and S. Li, “6G wireless communications: Vision and potential techniques,” IEEE Network, vol. 33, no. 4, pp. 70–75, 2019.

[4] K. David and H. Berndt, “6G vision and requirements: Is there any need for beyond 5G?” IEEE Vehicular Technology Magazine, vol. 13, no. 3, pp. 72–80, 2018.

[5] H. H. Meinel, “Evolving automotive radar — from the very beginnings into the future,” in The 8th European Conference on Antennas and Propagation (EuCAP 2014), 2014, pp. 3107–3114.

[6] C. Sun, “Recent advances and classification of radar technology,” Highlights in Science, Engineering and Technology, vol. 81, pp. 693–696, 2024.

[7] H. Yu, G. Yang, Y. Li, and F. Meng, “Design and analysis of multiple-input multiple-output radar system based on RF single-link technology,” Symmetry, vol. 10, no. 5, 2018. [Online]. Available: https://www.mdpi.com/2073-8994/10/5/130

[8] R. Fiengo and A. J. Adams, “Test and evaluation of radar systems operating in the modern electromagnetic spectrum,” IET Radar, Sonar Amp; Navigation, vol. 18, pp. 2189–2198, 2024.

[9] S. Iyer, A. Kalla, O. Lopez, and C. De Alwis, Intelligent Spectrum Management: Towards 6G. Wiley, 2025. [Online]. Available: https://books.google.ee/books?id=B484EQAAQBAJ

[10] C. Beckman and B. Lindmark, “The evolution of base station antennas for mobile communications,” in 2007 International Conference on Electromagnetics in Advanced Applications, 2007, pp. 85–92.

[11] S. Kutty and D. Sen, “Beamforming for millimeter wave communications: An inclusive survey,” IEEE Communications Surveys Tutorials, vol. 18, no. 2, pp. 949–973, 2016.

[12] M. Agiwal, A. Roy, and N. Saxena, “Next generation 5G wireless networks: A comprehensive survey,” IEEE Communications Surveys Tutorials, vol. 18, no. 3, pp. 1617–1655, 2016.

[13] J. S. Herd and M. D. Conway, “The evolution to modern phased array architectures,” Proceedings of the IEEE, vol. 104, no. 3, pp. 519–529, 2016.

[14] T. K. Sarkar, M. Salazar Palma, and E. L. Mokole, “Echoing across the years: A history of early radar evolution,” IEEE Microwave Magazine, vol. 17, no. 10, pp. 46–60, 2016.

[15] A. Bongers and J. L. Torres, “Technological change in US jet fighter aircraft,” Research Policy, vol. 43, no. 9, pp. 1570–1581, 2014.

[16] A. Brown, Active Electronically Scanned Arrays: Fundamentals and Applications, ser. IEEE Press. Wiley, 2021. [Online]. Available: https://books.google.ee/books?id=9odOEAAAQBAJ

[17] Q. K. Ud Din Arshad, A. U. Kashif, and I. M. Quershi, “A review on the evolution of cellular technologies,” in 2019 16th International Bhurban Conference on Applied Sciences and Technology (IBCAST), 2019, pp. 989–993.

[18] T. Chaloun, L. Boccia, E. Arnieri, M. Fischer, V. Valenta, N. J. G. Fonseca, and C. Waldschmidt, “Electronically steerable antennas for future heterogeneous communication networks: Review and perspectives,” IEEE Journal of Microwaves, vol. 2, no. 4, pp. 545–581, 2022.

[19] G. A. T. Warren L. Stutzman, Antenna Theory and Design. JOHN WILEY SONS, INC., 1998.

[20] A. van Bezooijen, M. A. de Jongh, C. Chanlo, L. C. H. Ruijs, F. van Straten, R. Mahmoudi, and A. H. M. van Roermund, “A GSM/EDGE/WCDMA adaptive series-LC matching network using RF-MEMS switches,” IEEE Journal of Solid-State Circuits, vol. 43, no. 10, pp. 2259–2268, 2008.

[21] H. M. Nemati, C. Fager, U. Gustavsson, R. Jos, and H. Zirath, “Design of varactor-based tunable matching networks for dynamic load modulation of high power amplifiers,” IEEE Transactions on Microwave Theory and Techniques, vol. 57, no. 5, pp. 1110–1118, 2009.

[22] V.-P. Kutinlahti, “Antenna mutual coupling and amplifier effects in transmission,” Doctoral thesis (article-based), School of Electrical Engineering, Aalto University, Apr. 2024.

[23] G. von Zengen, F. Büsching, W.-B. Pöttner, and L. Wolf, “Transmission power control for interference minimization in WSNs,” in 2014 International Wireless Communications and Mobile Computing Conference (IWCMC), 2014, pp. 74–79.

[24] N. Bankar and C. Patel, “Performance analysis of closed loop uplink power control schemes in cellular radio system,” in 2013 Nirma University International Conference on Engineering (NUiCONE), 2013, pp. 1–8.

[25] G. P. Gibiino, K. Lukasik, P. Barmuta, A. Santarelli, D. M. M.-P. Schreurs, and F. Filicori, “A two-port nonlinear dynamic behavioral model of RF PAs subject to wideband load modulation,” IEEE Transactions on Microwave Theory and Techniques, vol. 66, no. 2, pp. 831–844, 2018.

[26] H. Zargar, A. Banai, and J. C. Pedro, “A new double input-double output complex envelope amplifier behavioral model taking into account source and load mismatch effects,” IEEE Transactions on Microwave Theory and Techniques, vol. 63, no. 2, pp. 766–774, 2015.

[27] M. Romier, A. Barka, H. Aubert, J.-P. Martinaud, and M. Soiron, “Load-pull effect on radiation characteristics of active antennas,” IEEE Antennas and Wireless Propagation Letters, vol. 7, pp. 550–552, 2008.

[28] S. K. Dhar, A. Abdelhafiz, M. Aziz, M. Helaoui, and F. M. Ghannouchi, "A reflection-aware unified modeling and linearization approach for power amplifier under mismatch and mutual coupling," IEEE Transactions on Microwave Theory and Techniques, vol. 66, no. 9, pp. 4147–4157, 2018.

[29] M. Morris and M. Jensen, "Network model for MIMO systems with coupled antennas and noisy amplifiers," IEEE Transactions on Antennas and Propagation, vol. 53, no. 1, pp. 545–552, 2005.

[30] R. Maaskant, "Analysis of large antenna systems," Phd Thesis 2 (Research NOT TU/e / Graduation TU/e), Electrical Engineering, 2010.

[31] W. E. Fennouri, W. Saabe, and C. Mazière, "Advanced behavioral modeling of power amplifier for active antenna system simulation," in 2023 IEEE Conference on Antenna Measurements and Applications (CAMA), 2023, pp. 852–856.

[32] C. Fager, T. Eriksson, F. Barradas, K. Hausmair, T. Cunha, and J. C. Pedro, "Linearity and efficiency in 5G transmitters: New techniques for analyzing efficiency, linearity, and linearization in a 5G active antenna transmitter context," IEEE Microwave Magazine, vol. 20, no. 5, pp. 35–49, 2019.

[33] P. Gröschel, S. Zarei, C. Carlowitz, M. Lipka, E. Sippel, A. Ali, R. Weigel, R. Schober, and M. Vossiek, "A system concept for online calibration of massive MIMO transceiver arrays for communication and localization," IEEE Transactions on Microwave Theory and Techniques, vol. 65, no. 5, pp. 1735–1750, 2017.

[34] H. Barkhordar-Pour, J. G. Lim, A. B. Ayed, P. Mitran, and S. Boumaiza, "Active calibration approach addressing antenna mutual coupling and power amplifier output mismatch in fully digital MIMO transmitters," IEEE Microwave and Wireless Technology Letters, vol. 34, no. 6, pp. 813–816, 2024.

[35] D. M. Pozar, Microwave engineering; 4rd ed. Hoboken, NJ: Wiley, 2011.

[36] R. J. Mailloux, Phased Array Antenna Handbook, 3rd ed. USA: Artech House, Inc., 2017.

[37] T. A. Milligan, Arrays. John Wiley Sons, Ltd, 2005, ch. 3, pp. 102–135. [Online]. Available: https://onlinelibrary.wiley.com/doi/abs/10.1002/0471720615.ch3

[38] D. Root, J. Verspecht, J. Horn, and M. Marcu, X-Parameters: Characterization, Modeling, and Design of Nonlinear RF and Microwave Components, ser. The Cambridge RF and Microwave Engineering Series. Cambridge University Press, 2013. [Online]. Available: https://books.google.ee/books?id=Qf8PAQAAQBAJ

[39] F. M. Ghannouchi and M. S. Hashmi, "Load-pull techniques and their applications in power amplifiers design (invited)," in 2011 IEEE Bipolar/BiCMOS Circuits and Technology Meeting, 2011, pp. 133–137.

[40] P. Ramachandran, O. Bengtsson, and C. Beckman, "Impedance determination of terminal power amplifiers for optimal antenna matching using load-pull method," in 2009 IEEE International Workshop on Antenna Technology, 2009, pp. 1–4.

[41] M. Marchetti, M. J. Pelk, K. Buisman, W. C. E. Neo, M. Spirito, and L. C. N. de Vreede, "Active harmonic load–pull with realistic wideband communications signals," IEEE Transactions on Microwave Theory and Techniques, vol. 56, no. 12, pp. 2979–2988, 2008.

[42] A. Ferrero and M. Pirola, “Harmonic load-pull techniques: An overview of modern systems,” IEEE Microwave Magazine, vol. 14, no. 4, pp. 116–123, 2013.

[43] Maury Microwave, “MT1000 and MT2000 – Mixed-Signal Active Load Pull System (1.0 MHz to 67.0 GHz) And MT2001 System Software,” Feb. 2022, accessed: February 4, 2025. [Online]. Available: https://maurymw.com/wp-content/uploads/2023/11/4T-097.pdf

[44] S. C. Cripps, RF Power Amplifiers for Wireless Communications, Second Edition. USA: Artech House, Inc., 2006.

[45] Wolfspeed. (2022) Cghv59350 350 W, 5.2 - 5.9 GHz, 50-ohm input/output matched, GaN HEMT for C-Band radar systems. (accessed: 2024-08-29). [Online]. Available: https://www.mouser.com/catalog/specsheets/Cree_CGHV59350.pdf

[46] V.-P. Kutinlahti, A. Lehtovuori, and V. Viikari, “Amplifier-Antenna Array Optimization for EIRP by Phase Tuning,” in 2022 16th European Conference on Antennas and Propagation (EuCAP), 2022, pp. 1–5.

[47] D. Nopchinda and K. Buisman, “Measurement technique to emulate signal coupling between power amplifiers,” IEEE Transactions on Microwave Theory and Techniques, vol. 66, no. 4, pp. 2034–2046, 2018.

[48] A. M. Angelotti, G. P. Gibiino, T. S. Nielsen, D. Schreurs, and A. Santarelli, “Wideband active load–pull by device output match compensation using a vector network analyzer,” IEEE Transactions on Microwave Theory and Techniques, vol. 69, no. 1, pp. 874–886, 2021.

[49] V.-P. Kutinlahti, A. Lehtovuori, and V. Viikari, “Analyzing and Optimizing the EIRP of a Phase-Tunable Amplifier-Antenna Array,” IEEE Journal of Microwaves, vol. 3, no. 1, pp. 52–59, 2023.

[50] K.-C. Lee and T.-H. Chu, “Mutual coupling mechanisms within arrays of nonlinear antennas,” Electromagnetic Compatibility, IEEE Transactions on, vol. 47, pp. 963 – 970, 12 2005.

[51] J. H. Holland, Adaptation in Natural and Artificial Systems: An Introductory Analysis with Applications to Biology, Control and Artificial Intelligence. Cambridge, MA, USA: MIT Press, 1992.

[52] M. Mitchell, An Introduction to Genetic Algorithms. Cambridge, MA, USA: MIT Press, 1998.

[53] F. M. Barradas, L. C. Nunes, J. C. Pedro, and C. Erdmann, “A robust search algorithm of optimal driving signals for dual-input high power amplifiers,” in 2024 IEEE/MTT-S International Microwave Symposium - IMS 2024, 2024, pp. 543–546.

[54] D. E. Goldberg, Genetic Algorithms in Search, Optimization, and Machine Learning. New York: Addison-Wesley, 1989.

[55] M. Kansal, A. Cordero, S. Bhalla, and J. R. Torregrosa, “New fourth- and sixth-order classes of iterative methods for solving systems of nonlinear equations and their stability analysis,” Numerical Algorithms, vol. 87, pp. 1017–1060, 2020.

[56] R. Jackson, “Rollett proviso in the stability of linear microwave circuits—a tutorial,” IEEE Transactions on Microwave Theory and Techniques, vol. 54, no. 3, pp. 993–1000, 2006.

[57] N. Khalid, T. Abbas, and M. Bin Ihsan, “Power amplifier design using GaN HEMT in class-AB mode for LTE communication band,” in 2015 International Wireless Communications and Mobile Computing Conference (IWCMC), 2015, pp. 685–689.

[58] W. Sear and T. W. Barton, “Power-amplifier stabilization through out-of-band feedback,” IEEE Microwave and Wireless Components Letters, vol. 30, no. 8, pp. 768–771, 2020.

[59] L. Mori, I. Lizarraga, A. Anakabe, J.-M. Collantes, V. Armengaud, and G. Soubercaze-Pun, “Efficient calculation of stabilization parameters in RF power amplifiers,” IEEE Transactions on Microwave Theory and Techniques, vol. 68, no. 9, pp. 3686–3696, 2020.

[60] S. Chen, X. Li, J. Zhu, C. Zhang, W. Long, Y. Liu, S. Liu, and Z. Lu, “Reflection power suppression for solid state amplifiers with combiner optimization,” Review of Scientific Instruments, vol. 94, p. 034708, 03 2023.

[61] Vector Telecom Pty Ltd, Standard Gain Horn Antenna Datasheet, Vector Telecom Pty Ltd, March 2006, first release, Document date: 05-Mar-2006. [Online]. Available: https://www.vectortele.com/VT%20Datasheet/Antennas/Standard%20Gain%20Horn%20Antenna/VT70SGAH10NK.pdf

[62] D. Linkhart, Microwave Circulator Design, Second Edition, ser. Artech House microwave library. Artech House, 2014. [Online]. Available: https://books.google.ee/books?id=AutPAwAAQBAJ

[63] UIY. 4 to 8 GHz – drop in isolator. (accessed: 2024-08-29). [Online]. Available: https://www.uiy.com/Datasheet/UIYDI1220A.pdf

[64] S. Daneshmand, N. Sokhandan, M. Zaeri-Amirani, and G. Lachapelle, “Precise calibration of a GNSS antenna array for adaptive beamforming applications,” Sensors, vol. 14, no. 6, pp. 9669–9691, 2014. [Online]. Available: https://www.mdpi.com/1424-8220/14/6/9669

[65] M. G. Pralon, L. G. Pralon, D. Neudert-Schulz, and R. S. Thomä, “On the performance of real dual-polarized antenna arrays for 2D unconditional direction of arrival estimation,” in 2016 10th European Conference on Antennas and Propagation (EuCAP), 2016, pp. 1–5.

[66] K. Aggour and R. Negra, “Study of peak and backoff efficiency of different power amplifier classes in outphasing systems,” in 2013 European Conference on Circuit Theory and Design (ECCTD), 2013, pp. 1–4.

[67] K. H. An, O. Lee, H. Kim, D. H. Lee, J. Han, K. S. Yang, Y. Kim, J. J. Chang, W. Woo, C.-H. Lee, H. Kim, and J. Laskar, “Power-combining transformer techniques for fully-integrated CMOS power amplifiers,” IEEE Journal of Solid-State Circuits, vol. 43, no. 5, pp. 1064–1075, 2008.

[68] C. Fager, K. Hausmair, K. Buisman, K. Andersson, E. Sienkiewicz, and D. Gustafsson, “Analysis of nonlinear distortion in phased array transmitters,” in 2017 Integrated Nonlinear Microwave and Millimetre-wave Circuits Workshop (INMMiC), 2017, pp. 1–4.

[69] B. Gashi, S. Krause, R. Quay, C. Fager, and O. Ambacher, “Investigations of active antenna doherty power amplifier modules under beam-steering mismatch,” IEEE Microwave and Wireless Components Letters, vol. 28, no. 10, pp. 930–932, 2018.

[70] J.-M. Hannula, M. Kosunen, A. Lehtovuori, K. Rasilainen, K. Stadius, J. Ryynänen, and V. Viikari, “Performance analysis of frequency-reconfigurable antenna cluster with integrated radio transceivers,” IEEE Antennas and Wireless Propagation Letters, vol. 17, no. 5, pp. 756–759, 2018.

[71] A. R. Saleem, K. Stadius, J.-M. Hannula, A. Lehtovuori, M. Kosunen, V. Viikari, and J. Ryynänen, "A 1.5–5-GHz integrated RF transmitter front end for active matching of an antenna cluster," IEEE Transactions on Microwave Theory and Techniques, vol. 68, no. 11, pp. 4728–4739, 2020.

[72] J.-M. Hannula, J. Holopainen, and V. Viikari, "Further investigations on the behavior of a frequency reconfigurable antenna cluster," in 2017 11th European Conference on Antennas and Propagation (EUCAP), 2017, pp. 616–619.

[73] Hansen, "Linear connected arrays [coupled dipole arrays]," IEEE Antennas and Wireless Propagation Letters, vol. 3, pp. 154–156, 2004.

[74] J. T. Logan, S. S. Holland, D. H. Schaubert, R. W. Kindt, and M. N. Vouvakis, "A review of planar ultrawideband modular antenna (PUMA) arrays," in 2013 International Symposium on Electromagnetic Theory, 2013, pp. 868–871.

[75] W. Hallberg, D. Nopchinda, C. Fager, and K. Buisman, "Emulation of Doherty amplifiers using single- amplifier load–pull measurements," IEEE Microwave and Wireless Components Letters, vol. 30, no. 1, pp. 47–49, 2020.

[76] F. M. Barradas, P. M. Tomé, J. M. Gomes, T. R. Cunha, P. M. Cabral, and J. C. Pedro, "Power, linearity, and efficiency prediction for MIMO arrays with antenna coupling," IEEE Transactions on Microwave Theory and Techniques, vol. 65, no. 12, pp. 5284–5297, 2017.

[77] A. R. Vilenskiy, W.-C. Liao, R. Maaskant, V. Vassilev, O. A. Iupikov, T. Emanuelsson, and M. V. Ivashina, "Co-design and validation approach for beam-steerable phased arrays of active antenna elements with integrated power amplifiers," IEEE Transactions on Antennas and Propagation, vol. 69, no. 11, pp. 7497–7507, 2021.

[78] S. N. Nallandhigal and K. Wu, "Analysis and impact of port impedances on two-port networks and its application in active array antenna developments," IEEE Transactions on Microwave Theory and Techniques, vol. 69, no. 4, pp. 2357–2370, 2021.

[79] B. Goettel, J. Schäfer, A. Bhutani, H. Gulan, and T. Zwick, "In-antenna power-combining methods," in 2017 11th European Conference on Antennas and Propagation (EUCAP), 2017, pp. 2776–2730.

[80] T. O. Saarinen, J.-M. Hannula, A. Lehtovuori, and V. Viikari, "Combinatory feeding method for mobile applications," IEEE Antennas and Wireless Propagation Letters, vol. 18, no. 7, pp. 1312–1316, 2019.

[81] V.-P. Kutinlahti, A. Lehtovuori, and V. Viikari, "Optimizing RF efficiency of a vector-modulator-driven antenna array," IEEE Antennas and Wireless Propagation Letters, vol. 19, no. 12, pp. 2507–2511, 2020.

[82] S.-H. Li, S. S. H. Hsu, J. Zhang, and K.-C. Huang, "Design of a Compact GaN MMIC Doherty Power Amplifier and System Level Analysis With X-Parameters for 5G Communications," IEEE Transactions on Microwave Theory and Techniques, vol. 66, no. 12, pp. 5676–5684, 2018.

[83] D. T. Donahue, P. E. de Falco, and T. W. Barton, "Power amplifier with load impedance sensing incorporated into the output matching network," IEEE Transactions on Circuits and Systems I: Regular Papers, vol. 67, no. 12, pp. 5113–5124, 2020.

[84] C. F. Gonçalves, F. M. Barradas, L. C. Nunes, P. M. Cabral, and J. C. Pedro, "Quasi-load insensitive doherty pa using supply voltage and input excitation adaptation," IEEE Transactions on Microwave Theory and Techniques, vol. 70, no. 1, pp. 779–789, 2022.

[85] C. Balanis, Antenna Theory: Analysis and Design. Wiley, 2015. [Online]. Available: https://books.google.ee/books?id=PTFcCwAAQBAJ

[86] M. Alibakhshikenari, F. Babaeian, B. S. Virdee, S. Aïssa, L. Azpilicueta, C. H. See, A. A. Althuwayb, I. Huynen, R. A. Abd-Alhameed, F. Falcone, and E. Limiti, "A comprehensive survey on "various decoupling mechanisms with focus on metamaterial and metasurface principles applicable to SAR and MIMO antenna systems"," IEEE Access, vol. 8, pp. 192 965–193 004, 2020.

[87] D. Serghiou, M. Khalily, V. Singh, A. Araghi, and R. Tafazolli, "Sub-6 GHz dual-band 8 × 8 MIMO antenna for 5G smartphones," IEEE Antennas and Wireless Propagation Letters, vol. 19, no. 9, pp. 1546–1550, 2020.

[88] T. Wu and J. Wang, "Neutralization-line-based decoupling for miniaturized MIMO antenna array," Microwave and Optical Technology Letters, vol. 65, pp. 685–689, 2022.

[89] H. Yuan, S. Gong, P. Zhang, and X. Wang, "Wide scanning phased array antenna using printed dipole antennas with parasitic element," Progress in Electromagnetics Research Letters, vol. 2, pp. 187–193, 2008.

[90] E. Fritz-Andrade, H. Jardón-Aguilar, and J. A. Tirado-Méndez, "Mutual coupling reduction of two 2x1 triangular-patch antenna array using a single neutralization line for MIMO applications," Radioengineering, vol. 27, pp. 976–982, 2018.

[91] K. F. Warnick, Mutual Coupling and Multiple-Input Multiple-Output (MIMO) Communications. Hoboken, NJ, USA: John Wiley Sons, Ltd, 2021, ch. 9, pp. 257–285. [Online]. Available: https://onlinelibrary.wiley.com/doi/abs/10.1002/9781119565048.ch9

[92] H. C. Mohanta, A. Kouzani, and S. Mandal, "Reconfigurable Antennas and Their Applications," Universal Journal of Electrical and Electronic Engineering, vol. 6, pp. 239–258, 10 2019.

[93] C. G. Christodoulou, Y. Tawk, S. A. Lane, and S. R. Erwin, "Reconfigurable antennas for wireless and space applications," Proceedings of the IEEE, vol. 100, no. 7, pp. 2250–2261, 2012.

[94] Y. Liu, Q. Wang, Y. Jia, and P. Zhu, "A frequency- and polarization-reconfigurable slot antenna using liquid metal," IEEE Transactions on Antennas and Propagation, vol. 68, no. 11, pp. 7630–7635, 2020.

[95] A. Mabrouk, A. Ibrahim, and H. Hamed, "Reconfigurable antenna with frequency and beam switching using transformer oil and PIN-diode for microwave applications," Alexandria Engineering Journal, vol. 61, 07 2021.

[96] Y. Zhou, F. Zhu, S. Gao, Q. Luo, L.-H. Wen, Q. Wang, X. Yang, Y. Geng, and Z. Cheng, "Tightly Coupled Array Antennas for Ultra-Wideband Wireless Systems," IEEE Access, vol. 6, pp. 61 851–61 866, 2018.

[97] J. P. Doane, K. Sertel, and J. L. Volakis, "A wideband, wide scanning tightly coupled dipole array with integrated balun (TCDA-IB)," IEEE Transactions on Antennas and Propagation, vol. 61, no. 9, pp. 4538–4548, 2013.

[98] J.-M. Hannula, T. Saarinen, J. Holopainen, and V. Viikari, "Frequency reconfigurable multiband handset antenna based on a multichannel transceiver," IEEE Transactions on Antennas and Propagation, vol. 65, no. 9, pp. 4452–4460, 2017.

[99] T. Raj, R. Mishra, P. Kumar, and A. Kapoor, "Advances in MIMO antenna design for 5G: A comprehensive review," Sensors, vol. 23, no. 14, 2023. [Online]. Available: https://www.mdpi.com/1424-8220/23/14/6329

[100] I. Khan, K. Zhang, L. Ali, and Q. Wu, “Enhanced quad-port MIMO antenna isolation with metamaterial superstrate,” IEEE Antennas and Wireless Propagation Letters, vol. 23, no. 1, pp. 439–443, 2024.

[101] A. Kumar, A. Q. Ansari, B. K. Kanaujia, J. Kishor, and L. Matekovits, “A review on different techniques of mutual coupling reduction between elements of any MIMO antenna. part 1: DGSs and parasitic structures,” Radio Science, vol. 56, no. 3, pp. 1–25, 2021.

[102] K. AVX, “Thin-film RF/microwave directional couplers,” AVX Corporation, Datasheet CP0603, accessed 2024-03-27. [Online]. Available: https://datasheets.kyocera-avx.com/CP0603-Series.pdf

This thesis revolutionises RF front-end design by harnessing mutual coupling between antennas and amplifiers, moving beyond traditional component-centric approaches. It establishes a system-level co-design methodology, demonstrating significant improvements in frequency range, beam-steering, and power efficiency. This new paradigm promises more adaptable, efficient, and compact reconfigurable RF systems for 5G/6G communication and advanced radar.

Business, Economy
Art, Design, Architecture
Science, Technology
Crossover
Doctoral Theses

Aalto DT 134/2025

ISBN 978-952-64-2638-9
ISBN 978-952-64-2637-2 (pdf)

Aalto University
School of Electrical Engineering
Department of Electronics and Nanoengineering
aalto.fi